Supporting Information

Red-emitting fluorescence sensors for metal cations: the role of counter anions and sensing of SCN^- in biological materials

Lukas Lochman[†], Miloslav Machacek[†], Miroslav Miletin[†], Štěpánka Uhlířová[†], Kamil Lang[‡], Kaplan Kirakci[‡], Petr Zimcik[†], Veronika Novakova*[†]

[†] Faculty of Pharmacy in Hradec Kralove, Charles University, Akademika Heyrovskeho 1203, 50005, Hradec Kralove, Czech Republic

[‡] Institute of Inorganic Chemistry of the Czech Academy of Sciences, Husinec-Řež 1001, 250 68 Řež, Czech Republic

Corresponding Author

* Veronika Novakova: veronika.novakova@faf.cuni.cz, tel. +420 495 067 394; fax: +420 495 067 167.

Content

General

All of the organic solvents used in the synthesis were of analytical grade. Anhydrous butanol for the cyclotetramerization was freshly distilled from magnesium. Unsubstituted zinc phthalocyanine (ZnPc) was purchased from Sigma-Aldrich. All of the other chemicals for the syntheses were purchased from certified suppliers (*i.e.*, Sigma-Aldrich, TCI Europe, Acros, and Merck) and used as received. Deionized water was prepared using Millipore purification system (Merck–Millipore, Darmstadt, Germany). Thin layer chromatography was performed on Merck aluminum sheets coated with silica gel 60 F_{254}. Merck Kieselgel 60 (0.040–0.063 mm) was used for column chromatography. The melting points were measured on an Electrothermal IA9200-series digital melting-point apparatus (Electrothermal Engineering, Southend-on-Sea, Essex, Great Britain). The infrared spectra were measured on a Nicolet 6700 spectrophotometer in ATR mode. The ^{1}H and ^{13}C NMR spectra were recorded on a VNMR S500 NMR spectrometer. The chemical shifts are reported relative to $Si(CH_3)_4$ and were referenced to the signal of the solvent. The UV–Vis spectra were recorded using a Shimadzu UV-2600 spectrophotometer. Elemental analysis was carried out using a Vario Micro Cube Elemental Analyzer (Elementar Analysensysteme GmbH, Hanau, Germany). Fluorescence emission and excitation spectra were measured using a FS5 spectrofluorimeter (Edinburgh Instruments) equipped with an extension to the near-infrared region (photomultiplier R2658P). The samples and reference were excited at 580 nm (TPyzPz **4**$_B$ and **6**$_C$), 595 nm (TPyzPz **3**$_B$ and **5**$_C$, **7**$_D$, **8**$_D$) or 600 nm (TPyzPz **1**$_A$ and **2**$_A$). MS (APCI) was recorded in positive mode on Agilent 500 Ion Trap LC/MS (Agilent Technologies, Santa Clara, California, USA) by direct infusion into detector of the sample dissolved in methanol (MeOH). The MALDI-TOF mass spectra were recorded in a positive reflectron mode on a 4800 MALDI TOF/TOF mass spectrometer (AB Sciex, Framingham, MA, USA). The *trans*-2-[3-(4-tert-butylphenyl)-2-methyl-2-propenylidene]-malononitrile was used as a matrix. The instrument was calibrated externally with a five-point calibration using a Peptide Calibration Mix1 kit (LaserBio Laboratories, Sophia- Antipolis, France). Compounds 4-hydroxy-3,5-diisopropylbenzaldehyde[1], **10**[2], **13**[3] and **17**[4] and TPyzPzs **1**$_A$[3], **2**$_A$[2], **7**$_D$[5], **8**$_D$[5] and **9Zn** and **9H**[6] were prepared according the literature.

Synthesis of precursors

5-(1,4,7,10,13-pentaoxa-16-azacyclooctadecan-16-yl)-6-(2-(2-hydroxyethoxy)ethoxy)pyrazine-2,3-dicarbonitrile (11): 2,2'-oxydi(ethan-1-ol) (240 mg, 2.26 mmol) was dissolved in 1M NaOH in water (2.26 mL) and compound **10** (875 mg, 2.06 mmol) was added in tetrahydrofuran (THF) (15 mL). Reaction mixture was stirred for 1 hour at rt. Solvents were evaporated to dryness under reduced pressure and directly purified by column chromatography on silica with acetone as a mobile phase (R_f product = 0.19). Yellow oil, yield 801 mg (79 %). ^{1}H-NMR (acetone-d_6, 500 MHz) 3.52 – 3.55 (4H, m, crown-H); 3.61 – 3.65 (16H, m, crown-H); 3.82 (4H, t, J = 6 Hz); 3.89 – 3.91 (2H, m); 4.05 – 4.09 (4H, m) and 4.54 – 4.56 ppm (2H, m, CH_2OAr); ^{13}C-NMR (acetone-d_6, 125 MHz) 150.6, 148.1, 125.4, 116.5, 115.7, 115.4, 73.5, 73.4, 71.43, 71.30, 71.24, 71.23, 71.17, 69.0, 68.4, 62.00, 61.96 and 52.7 ppm; IR (ATR, cm^{-1}) 2918, 2850, 2226(CN), 1558, 1515, 1449, 1428, 1351, 1292, 1224, 1121, 925 and 759. MS (APCI$^+$) m/z: 496.3 $[M+H]^+$.

5-(1,4,7,10,13-pentaoxa-16-azacyclooctadecan-16-yl)-6-(2-(2-((tetrahydro-2H-pyran-3-yl)oxy)ethoxy)ethoxy)pyrazine-2,3-dicarbonitrile (12): Mixture of compound **11** (800 mg, 1.61 mmol), 3,4-dihydro-2*H*-pyran (543 mg, 6.46 mmol) and pyridinium *p*-toluenesulfonate (32 mg, 0.13 mmol) in chloroform (20 mL) was refluxed for 4 h. Colour changed to orange. Then, water was added (60 mL) and product was extracted with ethyl acetate (4×). Organic layers were collected, dried over anhydrous Na_2SO_4, evaporated to dryness and crude product was purified by column chromatography on silica with ethyl acetate/MeOH 8:1 as a mobile phase (R_f product = 0.47). Yellow oil, yield 510 mg (55 %). ^{1}H-NMR ($CDCl_3$, 500 MHz) 1.48 – 1.60 (4H, m, pyran-H); 1.67 – 1.84 (2H, m, pyran-H); 3.46 – 3.52 (1H, m, pyran-H); 3.61 – 3.68 (18H, m, crown-H); 3.75 (4H, t, J = 6 Hz); 3.81 – 3.86 (4H, m); 4.03 (4H, br s); 4.49 – 4.52 (2H, m, CH_2OAr) and 4.59 ppm (1H, t, J = 4 Hz, pyran-H); ^{13}C-NMR ($CDCl_3$, 125 MHz) 148.9, 146.6, 124.9, 115.8, 114.5, 114.2, 99.1, 77.3, 77.0, 76.7, 70.7, 70.5, 70.44, 70.43, 68.4, 67.3, 66.6, 62.4, 52.0, 30.5, 25.3 and 19.5 ppm; IR (ATR, cm^{-1}) 2965, 2866, 2226(CN), 1556, 1513, 1426, 1350, 1288, 1224, 1120, 1076, 1033, 987, 930, 872 and 814. MS (APCI$^+$) m/z: 580.3 $[M+H]^+$, 496.7 $[M-C_5H_8O]^+$.

5-((1,4,7,10-tetraoxacyclododecan-2-yl)methoxy)-6-chloropyrazine-2,3-dicarbonitrile (14): 5,6-dichloropyrazine-2,3-dicarbonitrile (500 mg, 2.51 mmol) was added to a mixture of 2-hydroxymethyl-12-crown-4 (570 mg, 2.76 mmol) and triethylamine (509 mg, 5.03 mmol) in THF (15 mL). Reaction mixture turned red, stirring continued for 2.5 h at rt. Solvent and triethylamine were evaporated under reduced pressure and crude product was directly purified by column chromatography on silica with ethyl acetate as a mobile phase (R_f poduct = 0.51). Yellow solid, yield 543 mg (59 %). Melting point 111.5-115.2 °C; ^{1}H-NMR (acetone-d_6, 500 MHz) 3.55 – 3.85 (14H, m, crown-H); 4.23 (1H, m, CH); 4.53 (1H, dd, J_1 = 7 Hz, J_2 = 7 Hz, CH_2OAr) and 4.69 ppm (1H, dd, J_1 = 4 Hz, J_2 = 4 Hz, CH_2OAr); ^{13}C-NMR (acetone-d_6, 125 MHz) 158.6, 143.4, 130.3, 124.7, 113.88, 113.86, 77.6,

72.4, 72.3, 71.4, 71.3, 71.17, 71.15 and 70.8 ppm; IR (ATR, cm^{-1}) 2927, 2864, 2242(CN), 1545, 1528, 1461, 1437, 1356, 1306, 1231, 1159, 1128, 1101, 1065, 1041, 1027, 976, 943, 919, 853 and 830.

5-((1,4,7,10-tetraoxacyclododecan-2-yl)methoxy)-6-(1,4,7,10-tetraoxa-13-azacyclopentadecan-13-yl)pyrazine-2,3-dicarbonitrile (15): 1-aza-15-crown-5 (596 mg, 2.72 mmol) in THF (5 mL) was added to a mixture of compound **14** (530 mg, 1.44 mmol) and anhydrous K_2CO_3 (397 mg, 2.87 mmol) in THF (10 mL). It turned orange immediately. Stirring continued for next 3h at rt. Solvent was evaporated under reduced pressure and crude product was purified by column chromatography on silica with ethyl acetate/acetone 1:1 as a mobile phase (R_f poduct = 0.21). Yellow oil, yield 743 mg (94 %). ^{1}H-NMR (acetone-d_6, 500 MHz) 3.56 – 3.89 (30H, m, crown-H); 3.98 – 4.04 (4H, m, crown-H); 4.11 (1H, m, CH); 4.42 (1H, dd, J_1 = 7 Hz, J_2 = 7 Hz, CH_2OAr) and 4.49 ppm (1H, dd, J_1 = 4 Hz, J_2 = 4 Hz, CH_2OAr); ^{13}C-NMR (acetone-d_6, 125 MHz) 150.7, 147.9, 125.4, 116.6, 115.6, 115.3, 77.6, 72.1, 71.7, 71.6, 71.4, 71.2, 71.14, 71.11, 70.8, 70.7, 70.3, 70.1, 69.4 and 54.1 ppm; IR (ATR, cm^{-1}) 2863, 2226(CN), 1558, 1522, 1508, 1428, 1354, 1289, 1255, 1223, 1120, 982, 926 and 840. MS (APCI$^+$) *m/z*: 552.3 $[M+H]^+$.

5,6-bis(4-(hydroxymethyl)-2,6-diisopropylphenoxy)pyrazine-2,3-dicarbonitrile (16): Compound **18** (1.203 g, 5.78 mmol) was dissolved in 1M NaOH in water (5.78 mL) with THF (10 mL) and 5,6-dichloropyrazine-2,3-dicarbonitrile (500 mg, 2.51 mmol) was added in THF (10 mL). Reaction mixture was stirred for 1 hour at rt. Solvents were evaporated, water was added (50 mL) and crude product was extracted to ethyl acetate (3×50 mL). Organic layers were collected, dried over anhydrous Na_2SO_4, and solvent was evaporated to dryness. Product was purified by column chromatography on silica with chloroform/acetone 9:1 as a mobile phase. White solid, yield 1.34 g (98 %). Melting point 245.4-245.8 °C; ^{1}H-NMR (aceton-d_6, 500 MHz) 7.37 (4H, s, ArH); 4.70 (4H, d, J = 5.9 Hz, CH_2OH); 4.29 (2H, t, J = 5.9 Hz, OH); 3.06 (4H, hept, J = 6.9 Hz, CH) and 1.23 ppm (24H, d, J = 7.0 Hz, CH_3); ^{13}C-NMR (aceton-d_6, 125 MHz) 152.3, 146.0, 142.6, 140.7, 125.3, 123.6, 114.3, 64.6 and 28.4 and 23.6 ppm; IR (ATR, cm^{-1}) 2967, 2933, 2872, 2241 (CN), 1607, 1548, 1508, 1465, 1444, 1405, 1385, 1362, 1334, 1271, 1232, 1188, 1157, 1114, 1089 and 1018.

4-(hydroxymethyl)-2,6-diisopropylphenol (18): $NaBH_4$ (303 mg, 8.0 mmol) was added dropwise to a solution of 4-hydroxy-3,5-diisopropylbenzaldehyde (1.5 g, 7.27 mmol) in MeOH (70 mL) and the mixture was left stirring for 30 min at rt. Reaction was acidified by diluted H_2SO_4, water was added (50 mL) and crude product was extracted to ethyl acetate (3×50 mL). Organic layers were collected, dried over anhydrous Na_2SO_4 and solvent was evaporated to dryness. Product was purified by column chromatography on silica with chloroform/acetone 9:1 as a mobile phase. Colourless oil, yield 1.42 g (94 %). ^{1}H-NMR (aceton-d_6, 500 MHz) 7.05 (2H, s, ArH); 7.00 (1H, s, ArOH); 4.53 (2H, dd, J_1 = 5.8 Hz, J_2 = 0.6 Hz, CH_2OH); 3.92 (1H, td, J_1 = 5.8 Hz, J_2 = 0.5 Hz, CH_2OH); 3.37 (2H, hept, J = 6.9 Hz, CH) and 1.22 ppm (12H, d, J = 6.9, 0.5 Hz, CH_3); ^{13}C-NMR (aceton-d_6, 125 MHz) 145.5, 130.4, 129.7, 117.8, 60.2, 22.5 and 18.4 ppm; IR (ATR, cm^{-1}) 2961, 2870, 1598, 1468, 1444, 1383, 1363, 1285, 1259, 1201, 1171, 1153, 1122, 1104, 1091, 1075 and 1004.

Synthesis of TPyzPzs

General method of statistical condensation: Precursors **12** or **15** (1 equiv) and **16** or **17** (3 equiv) with anhydrous zinc acetate (4 equiv) were dissolved under an argon atmosphere in a small amount of anhydrous pyridine (typically 1-3 mL). The reaction mixture was refluxed for 5h. Then, pyridine was partially evaporated followed by the addition of water (20 mL) to afford a dark suspension that was collected by filtration and washed several times with water. The target congener was isolated by column chromatography on silica. The mobile phases and quantities of starting compounds are provided below.

TPyzPz 3$_B$: Compound **12** (346 mg, 0.60 mmol), compound **17** (549 mg, 1.79 mmol), zinc acetate (438 mg, 2.39 mmol). Mobile phase: chloroform/MeOH/THF 10:0.5:1 (3×) (R_f product = 0.59), then with CHF/THF 10:1. Green oily solid, yield 48 mg (5 %). ^{1}H-NMR ($CDCl_3$/pyridine-d_5 3:1, 500 MHz) 1.21 – 1.51 (6H, m, pyran-H); 1.88 (9H, s, CCH_3); 1.90 (45H, s, CCH_3); 3.18 – 3.23 (1H, m, pyran-H); 3.32 – 3.43 (18H, m, crown-H); 3.47 – 3.61 (10H, m); 3.66 – 3.78 (4H, br s); 4.19 (2H, t, J = Hz, 4 Hz, CH_2OAr) and 4.34 ppm (1H, t, J = 4 Hz, pyran-H); ^{13}C-NMR ($CDCl_3$/pyridine-d_5 3:1, 125 MHz) 159.1, 158.6, 158.23, 158.20, 157.9, 157.8, 152.6, 152.4, 151.6, 151.5, 151.3, 150.80, 150.75, 150.50, 150.48, 148.8, 146.8, 144.9, 144.7, 144.5, 144.4, 144.3, 125.1, 115.9, 114.8, 114.5, 99.2, 71.0, 70.7, 70.6, 68.6, 67.5, 66.9, 62.5, 52.3, 31.1, 31.1, 30.86, 30.82, 30.8, 30.3, 30.1, 25.6 and 19.7 ppm. IR (ATR, cm^{-1}): 2972, 2867, 1744, 1556, 1514, 1442, 1427, 1362, 1350, 1286, 1255, 1225, 1123, 1077, 1033 and 978; MS (MALDI-TOF) *m/z*: 1561.4 $[M]^+$; 1584.4 $[M+Na]^+$; 3122.7 $[2M]^+$; λ_{max}(THF, ε) 654 (183 000), 596sh, 429sh and 377 nm (141 000 $dm^3mol^{-1}cm^{-1}$).

TPyzPz 4$_B$: Compound **12** (100 mg, 0.172 mmol), compound **16** (280 mg, 0.518 mmol), zinc acetate (127 mg, 0.69 mmol). Mobile phase: chloroform/MeOH/THF 20:3:2 (2×) (R_f product = 0.26). Blue oily solid, yield 30 mg (8 %). ^{1}H-NMR ($CDCl_3$/pyridine-d_5 3:1, 500 MHz) 0.99 – 1.15 (78H, m, CH_3 and pyran-H); 3.07 – 3.26 (12H, m, CH(CH_3)$_2$); 3.36 – 3.96 (34H, m, crown-H, CH_2O in lariat ether and CH_2O in pyran); 4.39 (1H, br s, OCHO); 4.60 (2H, s, CH_2OH); 4.65 (2H, s, CH_2OH); 4.69 (2H, s, CH_2OH); 4.87 (6H, s, CH_2OH); 5.27 (6H, br s, OH) and 7.21 – 7.39 ppm (12H, m, ArH, partially overlapped by solvent signal); ^{13}C-NMR ($CDCl_3$/pyridine-d_5 3:1, 125 MHz) 151.6, 147.3, 147.0, 142.6, 142.5, 141.00, 140.98, 140.8, 140.4, 140.3, 127.9, 124.2, 99.2, 70.5, 69.0, 66.9, 65.0, 62.4, 50.3, 44.7, 32.1, 31.6, 31.2, 30.8, 30.6, 30.4, 29.9, 29.7, 29.5, 28.5, 25.6, 23.7 ppm; IR (ATR, cm^{-1}) 2963, 2928, 2870, 1467,

1402, 1364, 1285, 1246, 1215, 1158, 1101, 1056, 1034 and 927; MS (MALDI-TOF) *m/z*: 2269.9 $[M]^+$; 2292.9 $[M+Na]^+$; 2308.8 $[M+K]^+$; λ_{max}(THF, ε) 637 (183 000), 579sh and 370 nm (175 000 $dm^3mol^{-1}cm^{-1}$).

TPyzPz 5C: Compound **15** (100 mg, 0.181 mmol), compound **17** (167 mg, 0.544 mmol), zinc acetate (133 mg, 0.725 mmol). Mobile phase: chloroform/MeOH/THF 10:0.5:1 (R_f product = 0.39), then twice with chloroform/MeOH/THF 10:0.25:1 (R_f product = 0.15). Green oily solid, yield 27 mg (9 %); ^{1}H-NMR ($CDCl_3$/pyridine-d_5 3:1, 500 MHz) 1.93 (9H, s, CCH_3); 1.947 (27H, s, CCH_3); 1.952 (18H, s, CCH_3); 3.37 – 4.28 (35H, m); 4.93 (1H, dd, J_1 = 6 Hz, J_2 = 6 Hz, CH_2OAr) and 5.02 ppm (1H, dd, J_1 = 5 Hz, J_2 = 5 Hz, CH_2OAr); ^{13}C-NMR ($CDCl_3$/pyridine-d_5 3:1, 125 MHz) 158.7, 158.2, 157.9, 157.8, 157.6, 157.4, 152.2, 151.9, 151.22, 151.20, 150.9, 150.49, 150.45, 150.20, 150.17, 148.1, 146.2, 144.55, 144.47, 144.3, 144.2, 144.04, 144.02, 143.97, 137.5, 124.7, 115.8, 114.4, 114.1, 76.7, 71.04, 71.02, 70.86, 70.81, 70.7, 70.45, 70.32, 70.23, 70.21, 70.05, 69.7, 69.4, 68.2, 53.6, 53.4, 51.06, 51.04, 51.03, 51.00, 50.97, 30.7, 30.6, 30.50 and 30.46 ppm; IR (ATR, cm^{-1}) 2916, 2863, 1524, 1470, 1446, 1427, 1362, 1252, 1138, 1101, 1045, 976, 847 and 784; MS (MALDI-TOF) *m/z*: 1533.3 $[M]^+$, 1556.3 $[M+Na]^+$; 3066.7 $[2M]^+$; 3089.6 $[2M+Na]^+$; λ_{max} (THF, ε): 653 (142 000), 594sh and 376 nm (100 000 $dm^3mol^{-1}cm^{-1}$).

TPyzPz 6C: Compound **15** (100 mg, 0.181 mmol), compound **16** (295 mg, 0.544 mmol), zinc acetate (133 mg, 0.725 mmol). Mobile phase: chloroform/MeOH/THF 10:1:1, then with chloroform/MeOH/THF 10:0.5:1 (R_f product = 0.40). Blue oily solid, yield 20 mg (5 %). ^{1}H-NMR ($CDCl_3$/pyridine-d_5 3:1, 500 MHz) 0.91 – 1.24 (72H, m, CH_3); 1.92 – 2.00 (12H, m, $CHCH_3$); 3.08 – 3.26 (4H, m, crown-H); 3.32 – 4.10 (30H, m, crown-H); 4.66 (2H, d, *J* = 7 Hz, CH_2OH); 4.83 – 4.89 (4H, m, CH_2OH); 5.03 (2H, s, CH_2OH); 5.18 – 5.28 (4H, m, CH_2OH); 5.35 – 5.52 (6H, m, OH) and 7.18 – 7.28 ppm (12H, m, ArH, partially overlapped by solvent signal); ^{13}C-NMR ($CDCl_3$/pyridine-d_5 3:1, 125 MHz) 171.3, 171.1, 148.4, 142.1, 141.9, 141.3, 141.1, 140.4, 128.0, 125.1, 124.9, 108.1, 107.9, 106.7, 98.4, 71.4, 70.8, 70.7, 70.5, 67.9, 67.6, 67.5, 67.1, 66.9, 65.4, 65.2, 65.1, 53.9, 30.0, 29.82. 29.78, 29.73, 28.7 and 28.6 ppm; IR (ATR, cm^{-1}) 2966, 2930, 2870, 1734, 1541, 1522, 1489, 1398, 1363, 1338, 1286, 1245, 1214, 1158, 1101, 1056 and 927; MS (MALDI-TOF) *m/z*: 2365.9 $[M+2Na+2K]^+$, 2388.9 $[M+3Na+2K]^+$; λ_{max} (THF, ε): 637 (128 000), 579sh and 365 nm (115 000 $dm^3mol^{-1}cm^{-1}$).

Always-ON control TPyzPz was isolated from synthesis of unsymmetrical TPyzPz sensors **4B** and **6C** as a first (dark blue) fraction in column chromatography. ^{1}H-NMR ($CDCl_3$/pyridine-d_5 3:1, 500 MHz) 0.88 – 1.11 (96H, m, CH_3); 3.07 (16H, hept, *J* = 6.8 Hz, $CHCH_3$); 4.85 (16H, s, CH_2OH) and 7.21 ppm (16H, s, ArH); ^{13}C-NMR ($CDCl_3$/pyridine-d_5 3:1, 125 MHz) 151.4, 149.8, 146.6, 142.4, 140.5, 139.4, 64.5, 28.0 and 23.2 ppm; MS (MALDI-TOF) *m/z*: 2233.0 $[M]^+$, 2256.0 $[M+Na]^+$, 2271.9 $[M+K]^+$

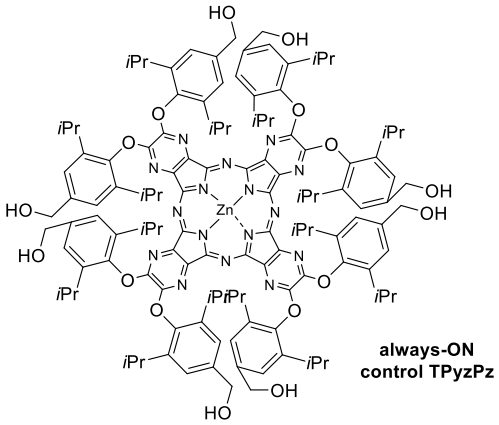

Alternative synthesis of cpd. **16**

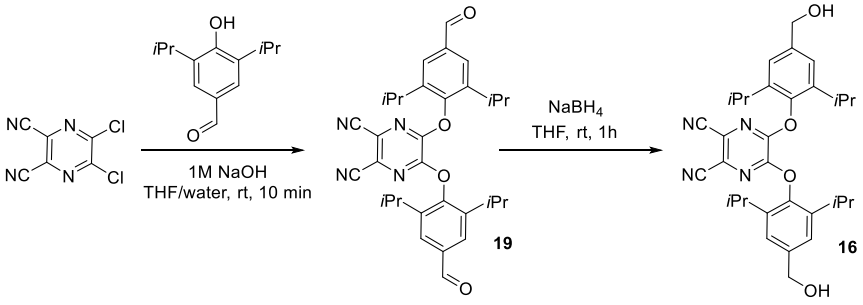

5,6-bis(4-formyl-2,6-diisopropylphenoxy)pyrazine-2,3-dicarbonitrile (19): 5,6-dichloropyrazine-2,3-dicarbonitrile (1.0 g, 5.02 mmol) in THF (20 mL) was added to 4-hydroxy-3,5-diisopropylbenzenaldehyde[1] (2.17 g, 10.56 mmol) in 1M NaOH (10.56 mL) at rt. Product was formed immediately. Product was extracted with chloroform/brine (50 mL, 3×), organic layers were collected, dried over anhydrous Na2SO4 and evaporated to dryness. Crude product was purified by column chromatography on silica with toluene/chloroform 1:1 (R_f=0.29) and crystallized from EtOH. White solid, yield 1.82 g (67 %). ^{1}H-NMR (aceton-d_6, 500 MHz) 10.12 (2H, s, CHO); 7.98 (4H, s, ArH); 3.16 (H, hept, J = 6.8 Hz, $CHCH_3$) and 1.31 ppm (24H, d, *J* = 6.7 Hz, CH3); 13C-NMR (aceton-d_6, 125 MHz) 192.3, 151.60, 151.57, 142.7, 136.9, 127.0, 125.8, 114.1, 28.5 and 23.0 ppm; IR (ATR, cm^{-1}) 2972, 2939, 2872, 2241(CN), 1698, 1598, 1550, 1432, 1386, 1363, 1263, 1277, 1224, 1175, 1158, 1114, 1097, 1007, 967, 945, 927 and 882.

5,6-bis(4-formyl-2,6-diisopropylphenoxy)pyrazine-2,3-dicarbonitrile (16): Compound **19** (100 mg, 0.19 mmol) and $NaBH_4$ (14 mg, 0.37 mmol) was dissolved in THF (5 mL) and stirred at rt for 1 h. Water (30 mL) was slowly added and solution was neutralized to weakly acidic pH by diluted H2SO4. Product was extracted with ethyl acetate (3×20 mL), organic layers were collected, dried over anhydrous Na_2SO_4 and evaporated to dryness. Crude product was purified by column chromatography on silica with chloroform/acetone 9:1 as an eluent. Yellow oil, yield 68 mg (60 %). NMR spectra corresponded well to the data of **16** prepared from 5,6-dichloropyrazine-2,3-dicarbonitrile and compound **18**.

Synthesis of nanoparticles (3$_B$@NPs)

First, 180 mg of Tween 80, 0.4 mL of butanol, and 10 mL of deionized water were added to a vial (40 mL) and vigorously stirred for 15 min. Then, a solution containing 0.1 mg of **3$_B$** and 0.1 mL of pyridine in 0.1 mL of DMF was added dropwise to the micellar solution. After one hour, 0.03 mL of triethoxyvinylsilane were added dropwise, and the emulsion was stirred for 3 days. The residual solvents and Tween 80 were removed by dialysing the nanoparticle dispersion against deionised water in a 12–14 kDa cut-off cellulose membrane (Spectrum Laboratories, Inc.) for 96 h where the water was changed every 24 hours. The average hydrodynamic diameter was 7 nm with a low polydispersity (PDI = 0.15). (Fig. S12).

Methods

Fluorescence titration experiments of NP: A total of 2.5 mL of a **3B@NP** (c ~ 1 μM) stock solution in water was transferred to a 10 × 10 mm fluorescence quartz cell, and the absorption and emission spectra (λ_{exc} = 595 nm) were recorded. Then, defined amounts (typically 5-50 μL) of the aqueous analyte stock solution (1 M) were subsequently added and the absorption and emission spectra were measured after each addition. The fluorescence intensity was corrected to the same absorption at the excitation wavelength and plotted as a function of the analyte concentration.

Job's method of continuous variation: To avoid any influence from the dilution by MeOH, stock solutions of TPyzPz (100 μM) in THF and of KSCN (1 mM) in MeOH were prepared. A series of fluorescence measurements with different TPyzPz/KSCN ratios (20 measurements ranging between 1:5 to 5:1 ratios) was performed as follows: an appropriate amount of THF that resulted in a the total volume of the solution being 2.0 mL after addition of stock solutions of TPyzPz and KSCN was transferred to a 10 × 10 mm fluorescence quartz optical cell. A stock solution containing compound TPyzPz was added, and the fluorescence emission spectrum was recorded (λ_{exc} = 591 nm) and obtained area under the emission curve was considered as Fo. An appropriate amount of the KSCN stock solution was added to yield a total concentration of components 10 μM ([TPyzPz] + [K^+] = 10 μM), and the fluorescence emission spectrum was recorded under the same conditions as before (F_{KSCN}). The final stoichiometry of the TPyzPz/KSCN complex was determined from the Job´s plot constructed from the dependence of F_{KSCN}-Fo on [TPyzPz]/([TPyzPz]+[KSCN]).

Cells for *in vitro* sensing: The human cervical carcinoma (HeLa) cell line was purchased from the American Type Cell Culture Collection (ATCC; USA). The cells were cultured in Dulbecco's Modified Eagle's Medium (DMEM) without phenol red (Lonza, Belgium) and supplemented with 10 % FBS (Sigma), 1 % penicillin/streptomycin solution (Lonza), 10 mM HEPES buffer (Sigma, Germany), and 4 mM L-glutamine (Lonza), further referred to as the cell culture medium. The cells were cultured in 75 cm^2 tissue culture flasks (TPP, Switzerland) and maintained in a CO2 incubator at 37 °C in a humidified atmosphere of 5 % CO_2 and subcultured every 3–4 days.

Toxicity assessment: HeLa cells were seeded on 96-well plates (TPP, Switzerland) at a density of 7.5 × 103 cells per well. The cells were allowed to grow in a CO2 incubator for 24 hours prior to **4B** addition. A wide concentration range (10 nM to 10 000 nM) was used. After 24 incubation with the sensor in the absence of light, the cellular viability was evaluated using a neutral red (Sigma) uptake assay. The optical density was measured using a Tecan Infinite 200 M plate reader (Tecan, Austria), and the viability is presented as a percentage (± standard deviation) of the untreated control cells incubated under the same experimental conditions (100 %). Prior to the cellular viability assessment, each sample was observed using an inverted microscope to detect the presence of precipitated **4B**. The solubility limit in the cell culture media was determined to be 5 µM.

Subcellular localization: The cells incubated with 1 µM **4B** for 12 hours were washed with prewarmed serum free medium and stained with 0.2 µM MitoTracker Green FM (Molecular Probes) and 0.25 µM LysoTracker Blue DND-22 (Molecular Probes) in serum free medium containing KSCN (10 mM) for 20 min. After staining, the cells were washed twice with prewarmed serum free medium for 5 min to wash out any free fluorescent probe. The sample was imaged using a Nikon Eclipse Ti-E fluorescence microscope as described above. DAPI, FITC, and Cy_5 filter sets were used for visualization of lysosomes, mitochondria and **4B**, respectively.

Cellular uptake: HeLa cells were seeded into 6 cm Petri dishes (TPP) at a density of 5.0×10^5 cells per dish. The medium was removed 24 h after the seeding, and 5 mL of a 0.5 µM solution of always-ON control TPyzPz in a cell culture medium was added (prepared from a 10 mM stock solution in DMSO). The cells were washed twice with 5 mL of prewarmed phosphate-buffered saline (PBS; Sigma) after 0, 0.5, 1, 2, 4, 6, 12 and 24 h. PBS (5 mL) was added, and the cells were scraped and transferred to 15 mL centrifugation tubes (TPP), petri dishes were washed again with PBS (5 mL) to harvest all the remaining cells and centrifuged for 5 min at 70 g. Pellets were left to dry and 500 µL of DMSO was added and cells were resuspended. Lysis of the cells was performed overnight at –80 °C. The samples were quickly thawed at 37 °C and frozen at –80 °C for an additional 2 h. The fluorescence of the thawed samples (λ_{ex} = 369 nm, λ_{em} = 640 nm) was measured using an FS5 spectrofluorimeter. Nonspecific fluorescence was excluded by the control experiments. A calibration curve was constructed using dilutions of the TPyzPz into the cell lysate prepared as described above. The uptake experiments were performed in duplicate. The amounts of protein in the samples were assessed using the BCA (bicinchoninic acid) method. A calibration curve was created using 10 µL of bovine serum albumin dissolved in MQ water at concentrations of 0, 50, 100, 200, 400, 600, 800, 1000 and 2000 µg/mL. A working solution of BCA (4% $CuSO_4 \cdot 6H_2O$ mixed *ad hoc* with BCA stock solution at a 1:50 ratio) was added to 10 µL of the samples. 10 µL of DMSO or MQ water was added to a calibration curve or samples, respectively. Absorbance (562 nm) was measured after 30 min incubation at 37 °C using a Tecan Infinite M 200 plate reader. Experiments were performed in dark the entire time.

Absorption spectra

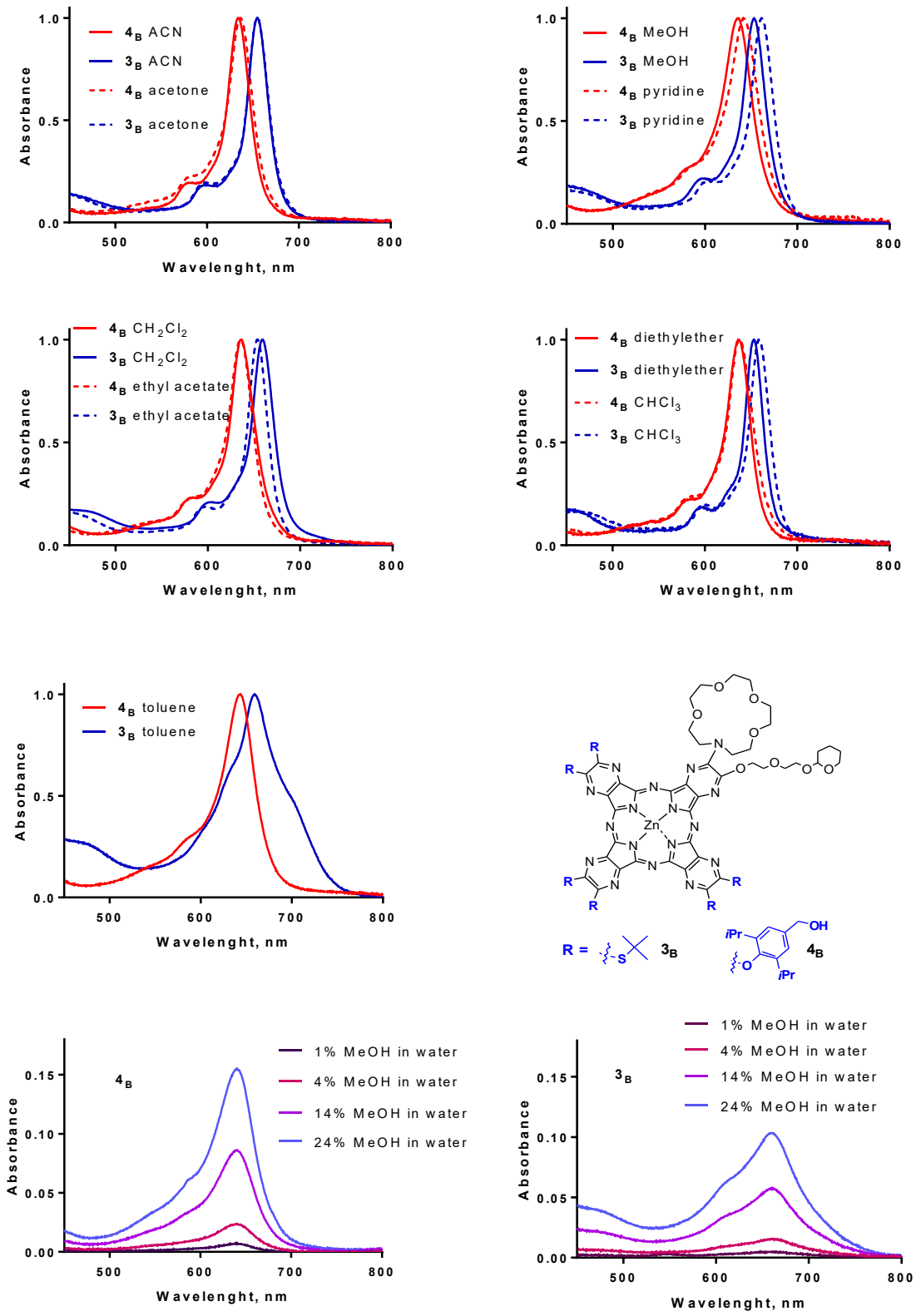

Fig. S1: Absorption spectra of TPyzPzs $\mathbf{3_B}$ or $\mathbf{4_B}$ (1µ M) in different solvents.

Titration experiments – the role of the structure of recognition moiety

Table S1: Sensing properties of studied sensors in THF (analytes in the form of triflates)

		1_A	**2_A**	**3_B**	**4_B**	**5_C**	**6_C**	**7_D**	**8_D**
Free form	Φ_F (F_{max})	0.012 (666)	0.011 (667)	0.012 (667)	0.014 (643)	0.017 (666)	0.010 (646)	0.00039 (670)	0.0010 (673)
	λ_{max} (ε)	654 (144 000)	654 (165 000)	654 (183 000)	637 (183 000)	653 (142 000)	637 (128 000)	654 (158 000)	654 (152 000)
Na^+	Φ_F	0.012	0.015	0.013	0.027	0.035	0.021	0.0013	0.0050
	FEF (K_A)	1.0	1.4	1.1	1.9	2.0 (30)	2.1 (30)	3.3	5.0
K^+	Φ_F	0.013	0.044	0.092	0.086	0.14	0.090	0.0055	0.0050
	FEF (K_A)	1.1	4.0 (540)	7.4 (490)	6.0 (10 800)	7.9 (750)	8.9 (4 100)	14	5.0
Li^+	Φ_F	0.007	0.011	0.012	0.013	0.017	0.0081	0.0004	0.0008
	FEF	< 1 *	< 1 *	< 1 *	< 1 *	< 1 *	< 1 *	< 1*	< 1*
NH_4^+	Φ_F	0.007	0.011	0.029	0.023	0.016	0.0095	0.0004	0.0007
	FEF	< 1 *	1.0	2.3	1.6	< 1 *	< 1 *	< 1 *	< 1*
Ca^{2+}	Φ_F	0.008	0.048	0.042	0.018	0.016	0.0095	0.0022	0.0008
	FEF (K_A)	< 1 *	4.4 (42 800)	3.4	1.2	< 1 *	1.0	5.5	< 1*
Ba^{2+}	Φ_F	0.008	0.23	0.26	0.21	0.21	0.18	0.17	0.074
	FEF (K_A)	< 1 *	22 (1 700))	21 (10 100)	15 (53 100)	13 (1 200)	18 (18 500)	439 (69)	74
Mg^{2+}	Φ_F	0.008	0.011	0.021	0.012	0.015	0.028	0.0079	0.036
	FEF	< 1 *	1.0	< 1 *	1.0	< 1 *	2.8	20	36

*λ_{max} - absorption maximum (nm), ε - molar absorption coefficient ($mol^{-1}dm^{-3}cm^{-1}$), F_{max} - fluorescence emission maximum, Φ_F fluorescence quantum yield, FEF - fluorescence enhancement factor for complete binding, K_A (in M^{-1}) - apparent association constant of the formation of analyte-sensor complex (determined from Φ_F); *negligible decrease in FEF due to increase of polarity of medium*

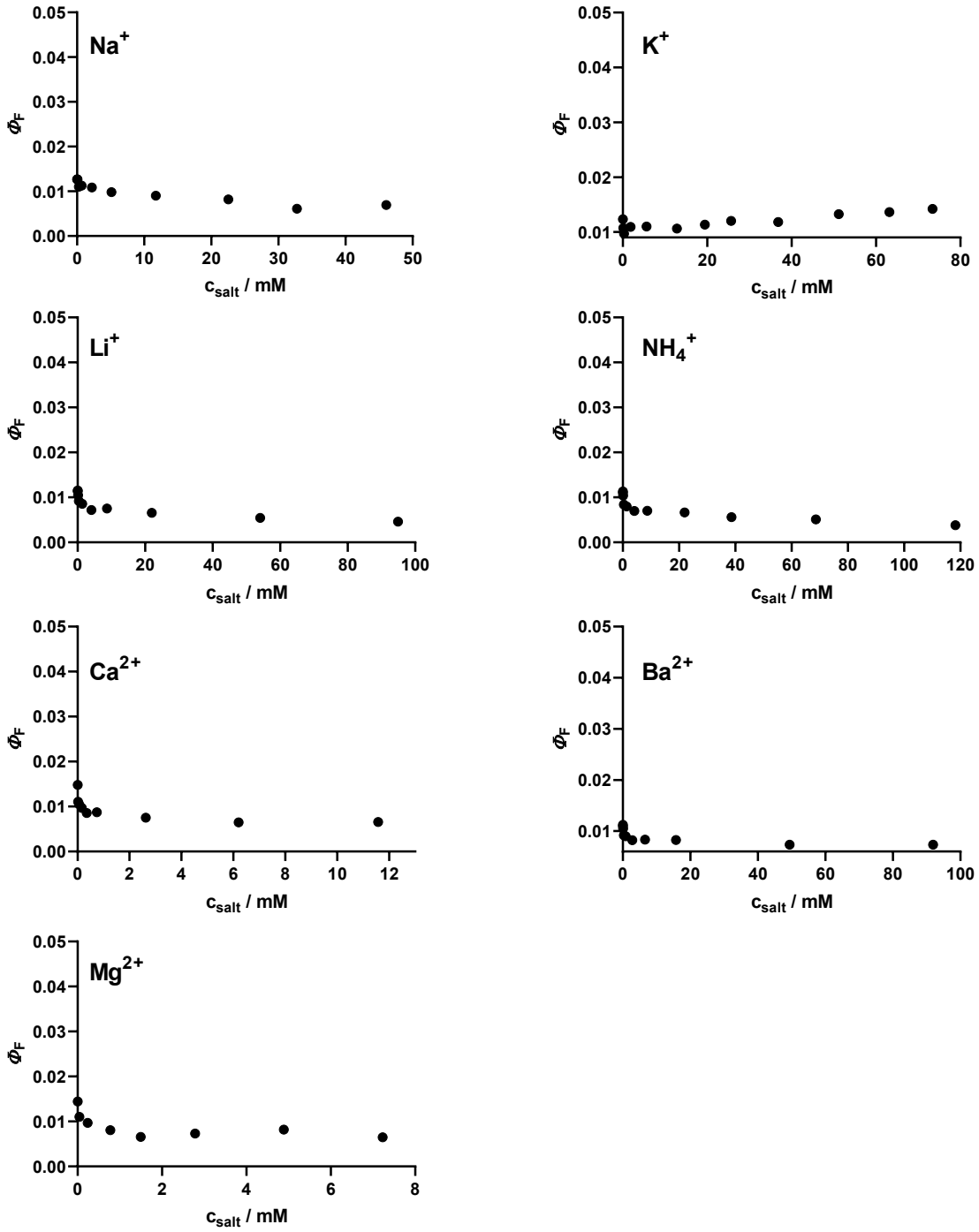

Fig. S2: Dependence of Φ_F of **1**$_A$ in THF on the concentration of added salt (in the form of triflate). The solid lines are the least-square fits to the experimental points

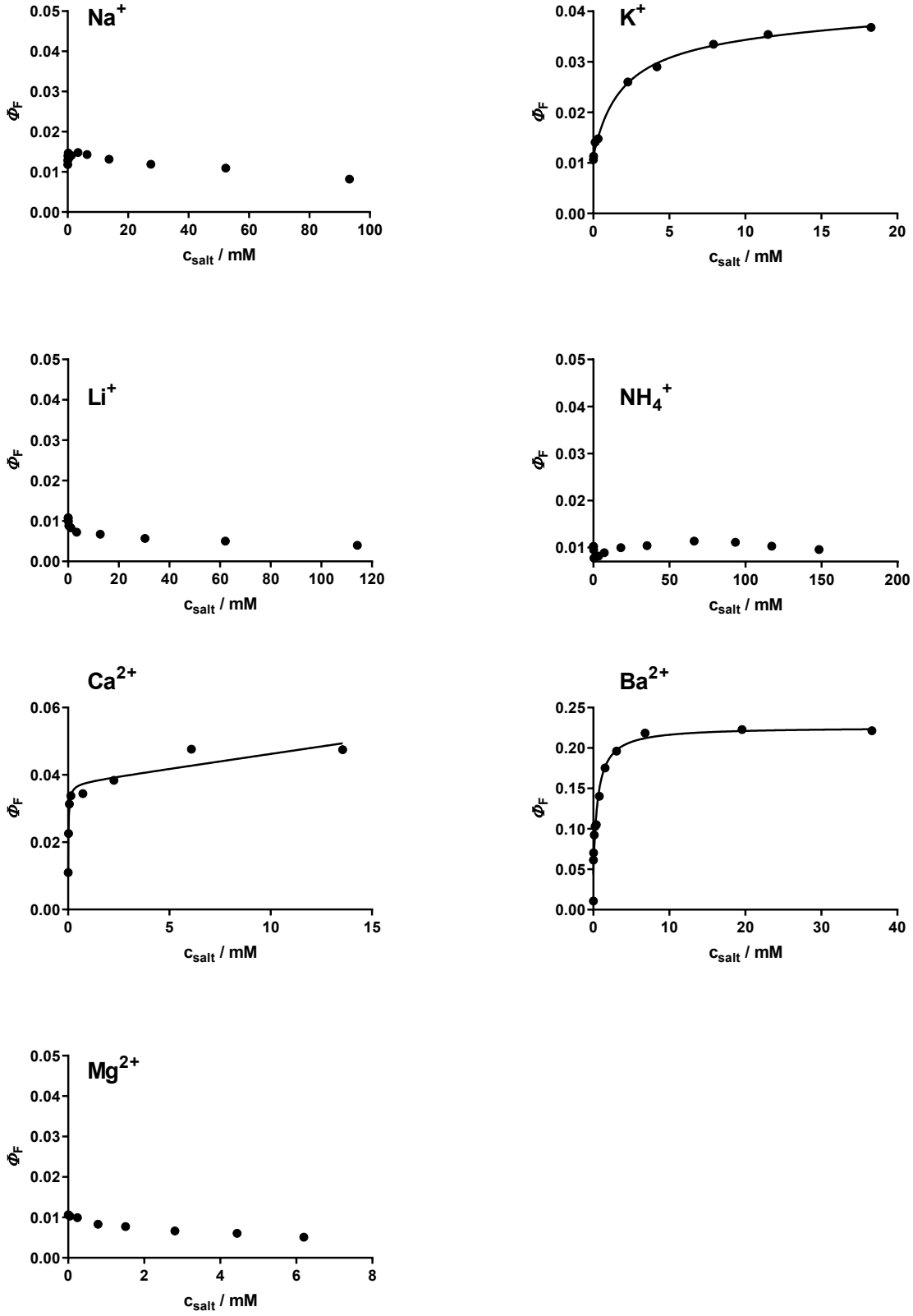

Fig. S3: Dependence of Φ_F of **2**$_A$ in THF on the concentration of added salt (in the form of triflate). The solid lines are the least-square fits to the experimental points.

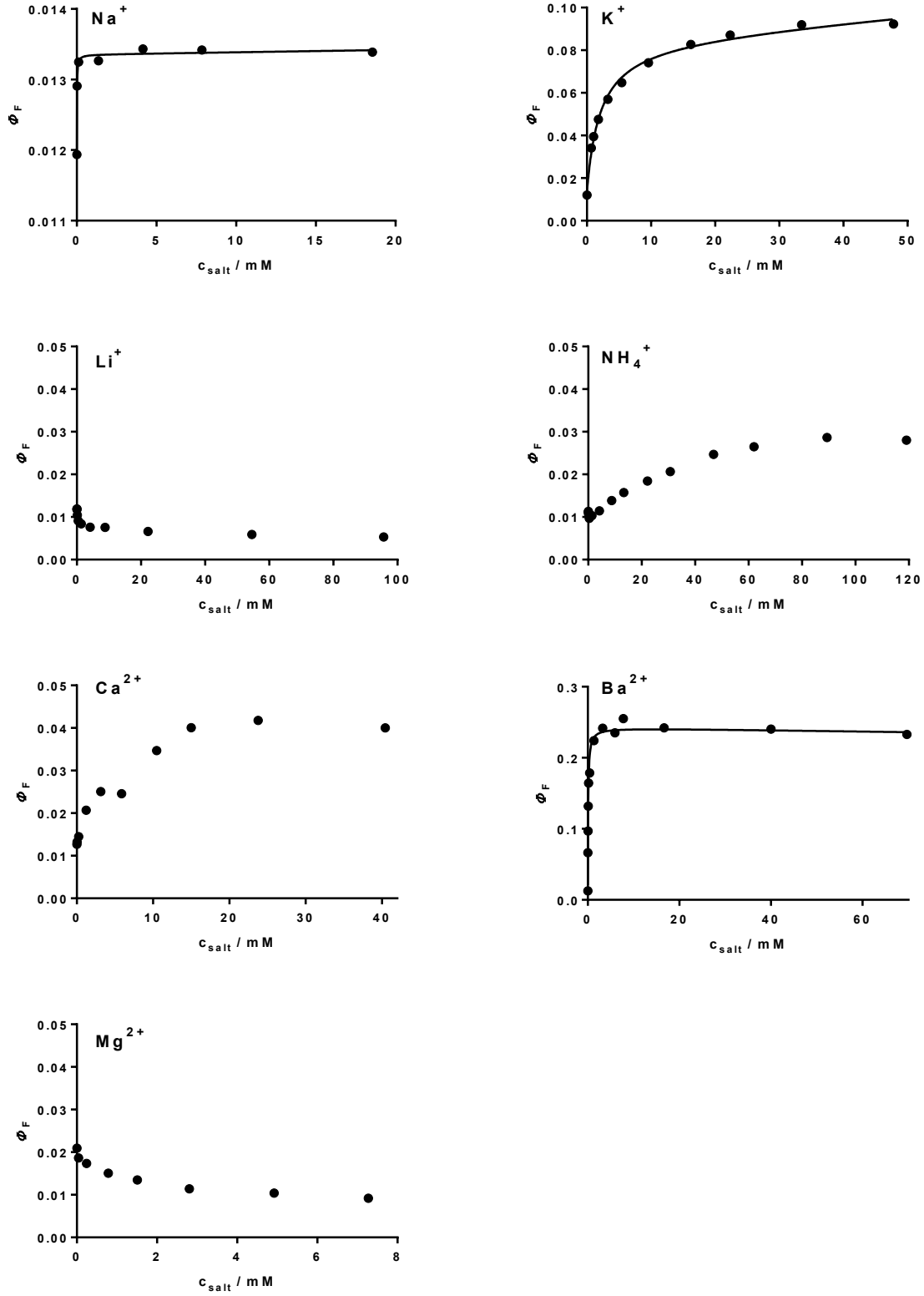

Fig. S4: Dependence of Φ_F of **3$_B$** in THF on the concentration of added salt (in the form of triflate). The solid lines are the least-square fits to the experimental points.

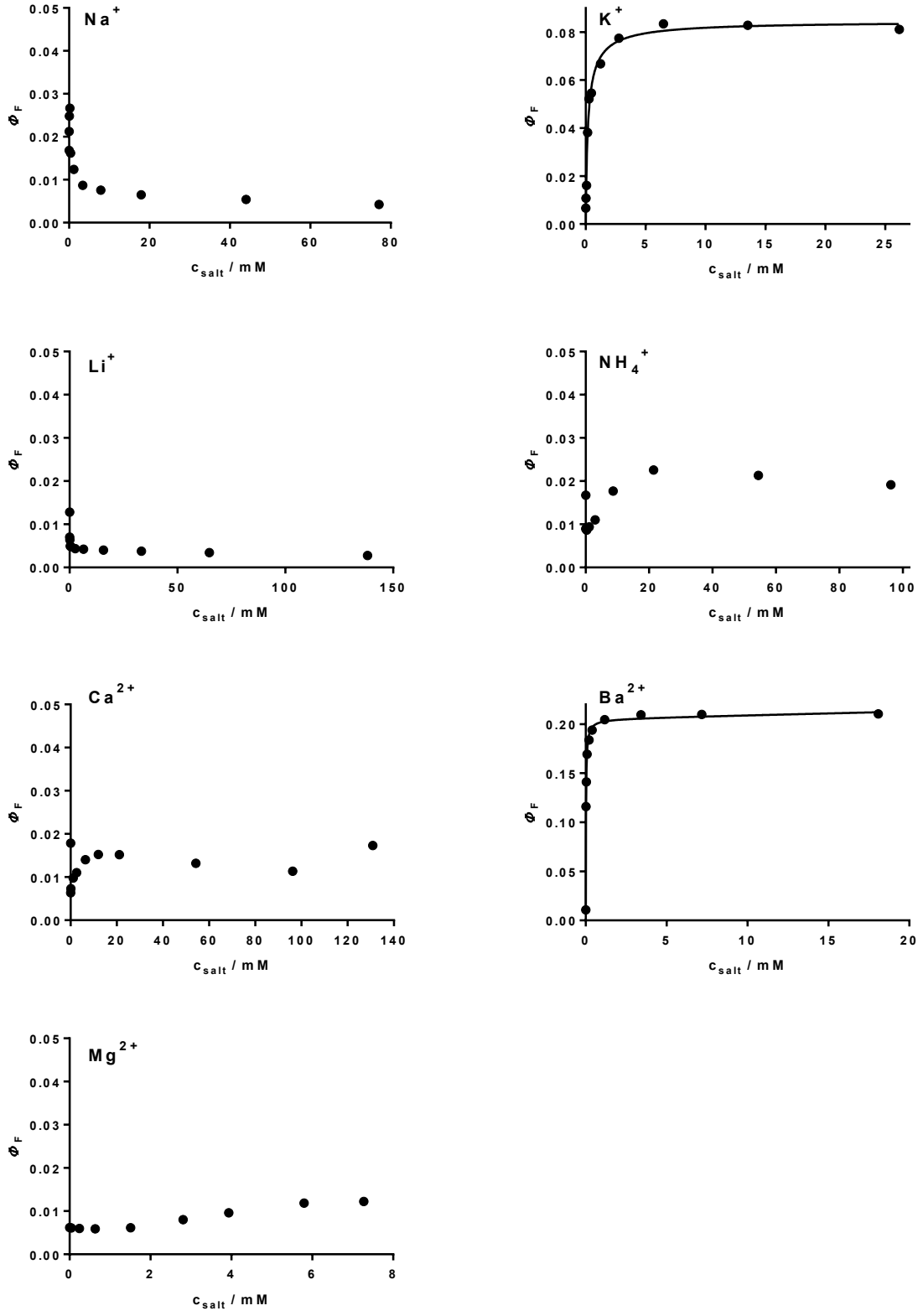

Fig. S5: Dependence of Φ_F of **4**$_B$ in THF on the concentration of added salt (in the form of triflate). The solid lines are the least-square fits to the experimental points.

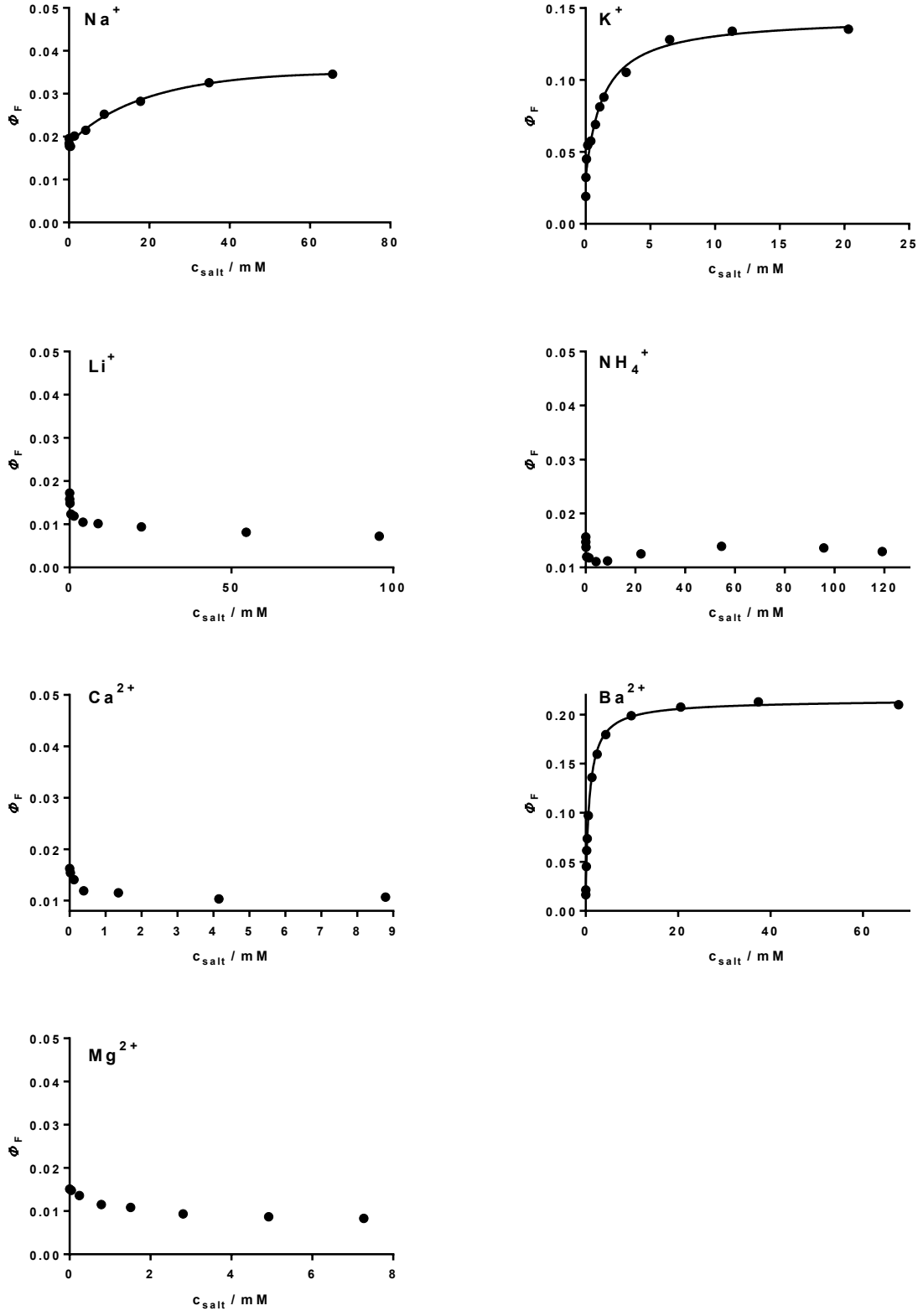

Fig. S6: Dependence of Φ_F of **5c** in THF on the concentration of added salt (in the form of triflate). The solid lines are the least-square fits to the experimental points.

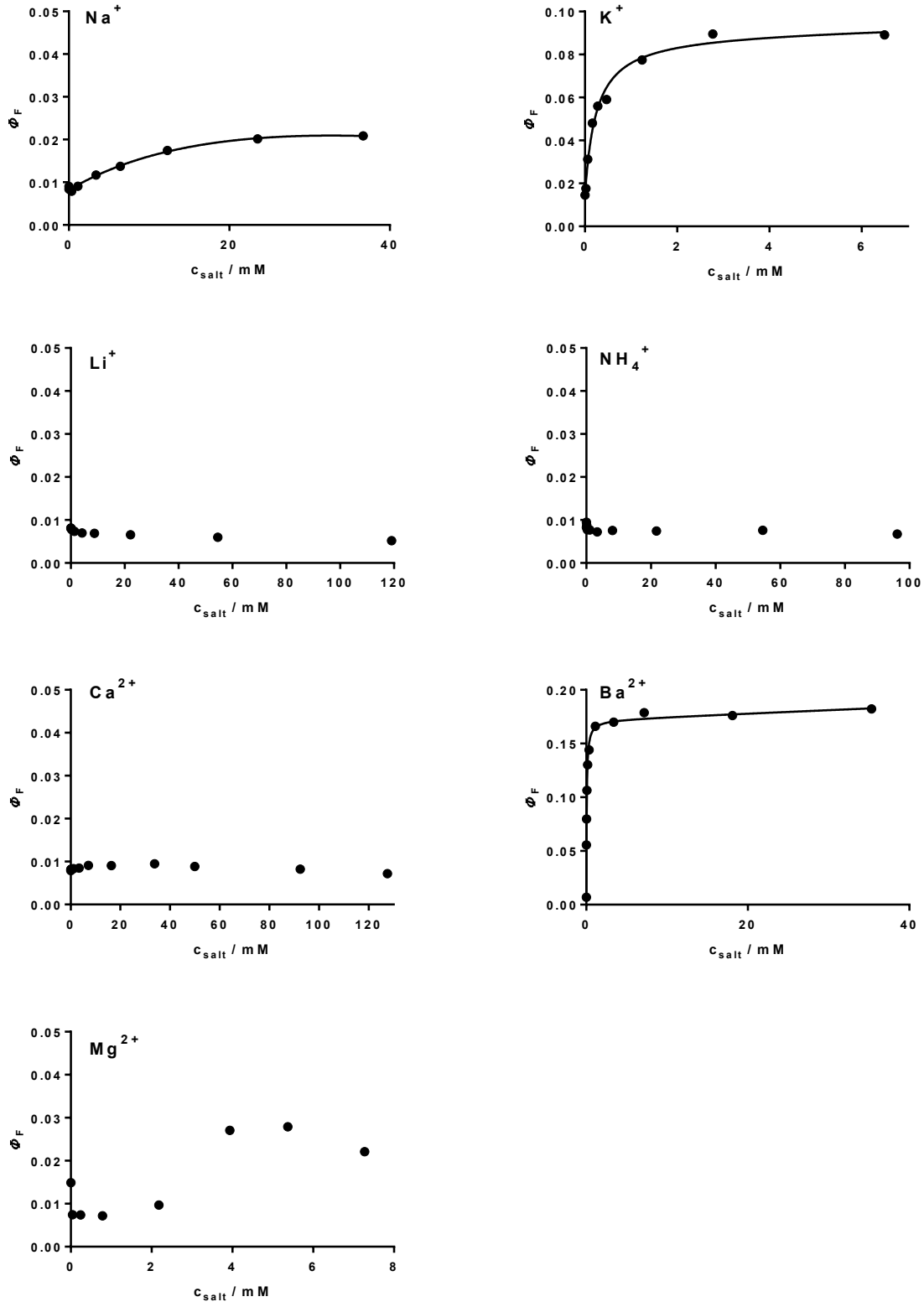

Fig. S7: Dependence of Φ_F of **6c** in THF on the concentration of added salt (in the form of triflate). The solid lines are the least-square fits to the experimental points.

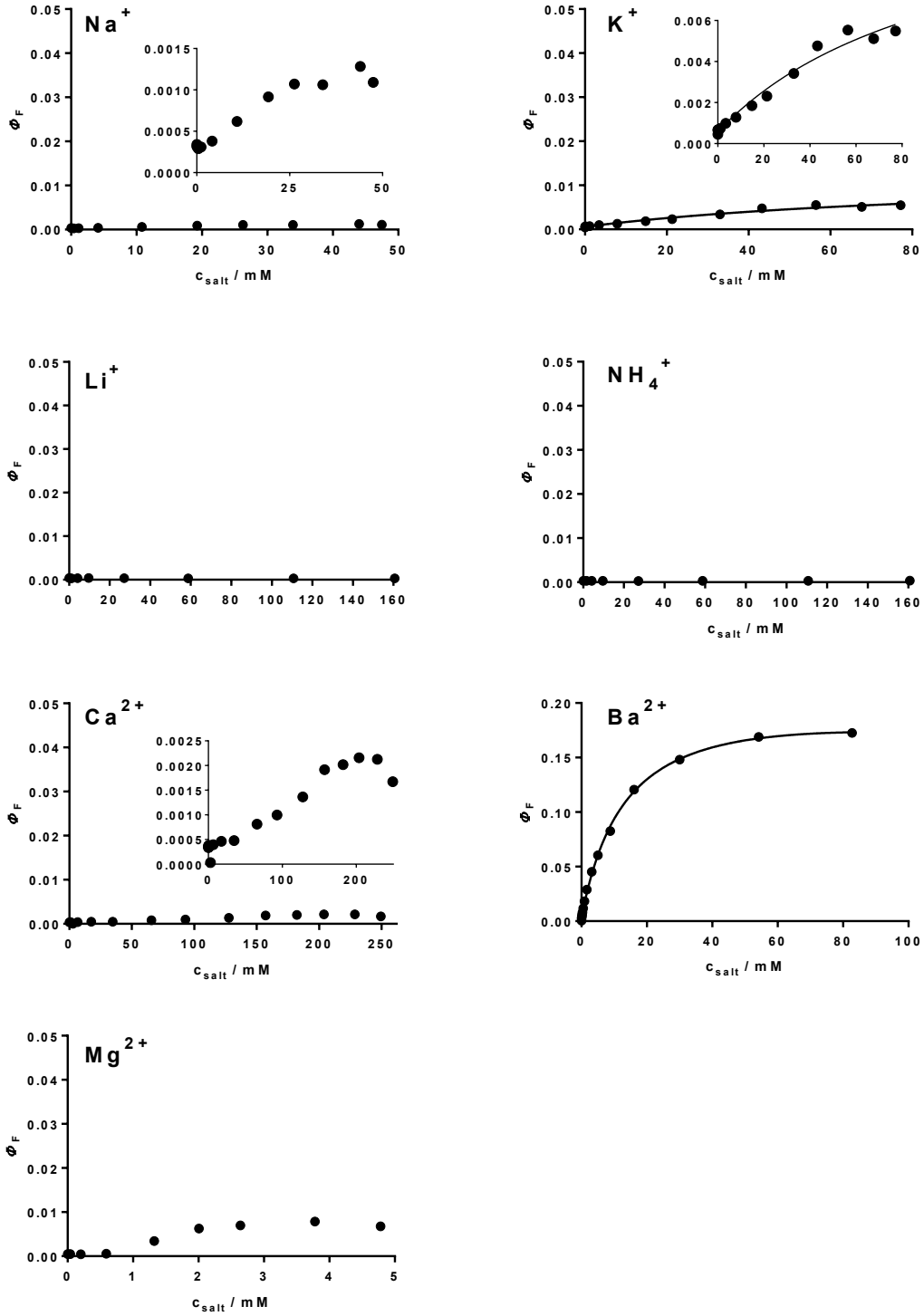

Fig. S8: Dependence of Φ_F of **7$_D$** in THF on the concentration of added salt (in the form of triflate). The solid lines are the least-square fits to the experimental points.

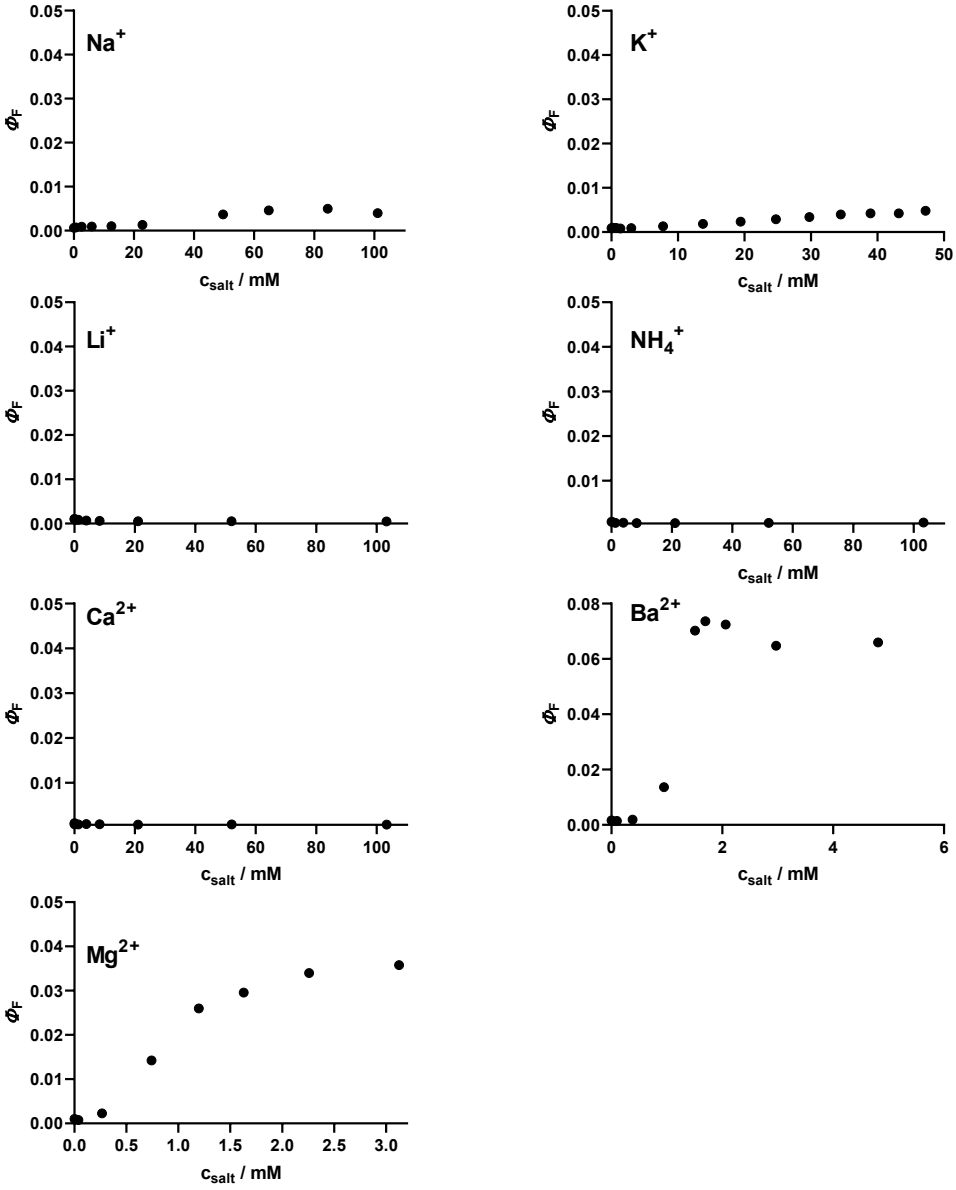

Fig. S9: Dependence of Φ_F of **8**$_D$ in THF on the concentration of added salt (in the form of triflate).

Titration experiments - the role of counter anion

Table S2: Effect of the counter anion of sodium salt on the sensing properties of sensors in THF

		1_A	**3_B**	**5_C**	**8_D**
Free form	**Φ_F (F_{max})**	0.012 (667)	0.013	0.017 (666)	0.00060 (670)
	λ_{max} (ε)	654 (156 000)	654 (183 000)	653 (142 000)	654 (152 000)
$CF_3SO_3^-$	**Φ_F (FEF)**	0.013 (1.1)	0.014 (1.1)	0.035 (2.0)	0.0050 (8.3)
ClO_4^-	**Φ_F (FEF)**	0.024 (2.0)	0.016 (1.2)	0.038 (2.3)	0.036 (61.0)
SCN^-	**Φ_F (FEF)**	0.11 (9.1)	0.14 (10.8)	0.15 (9.2)	0.053 (88.2)
NO_3^-	**Φ_F (FEF)**	0.012 (1.0)	0.016 (1.2)	0.017 (1.0)	0.00061 (1.0)
Br^-	**Φ_F (FEF)**	0.019 (1.6)	0.038 (2.9)	0.031 (1.9)	0.0031 (5.2))

λ_{max} - Q band absorption maximum (nm), ε - molar absorption coefficient ($mol^{-1}dm^{-3}cm^{-1}$), F_{max} - position of fluorescence emission maximum, Φ_F fluorescence quantum yield (unsubstituted zinc phthalocyanine was used as a reference (Φ_F = 0.32 in THF[7])), FEF - fluorescence enhancement factor for complete binding (*i.e.*, ratio of fluorescence intensity between ON and OFF state).

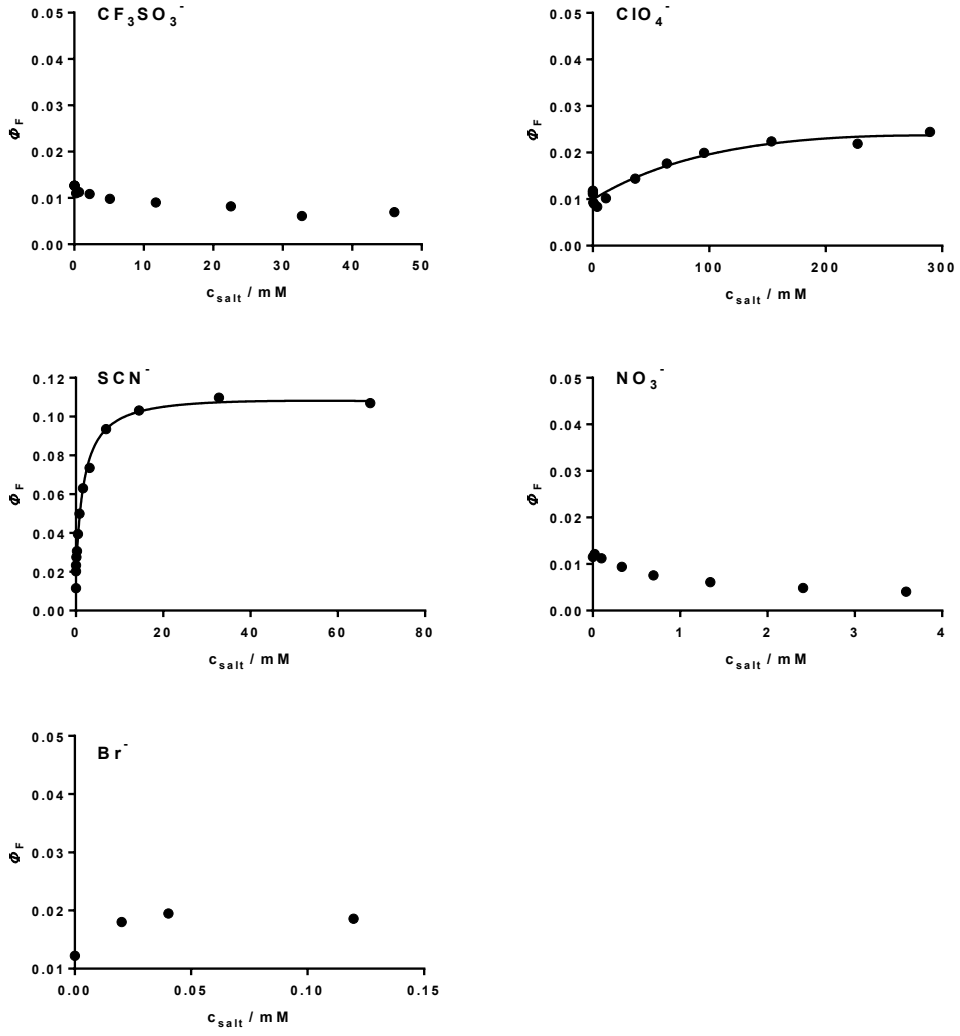

Fig. S10: The role of counter anions: Dependence of Φ_F of **1_A** in THF on the concentration of added sodium salt. The solid lines are the least-square fits to the experimental points.

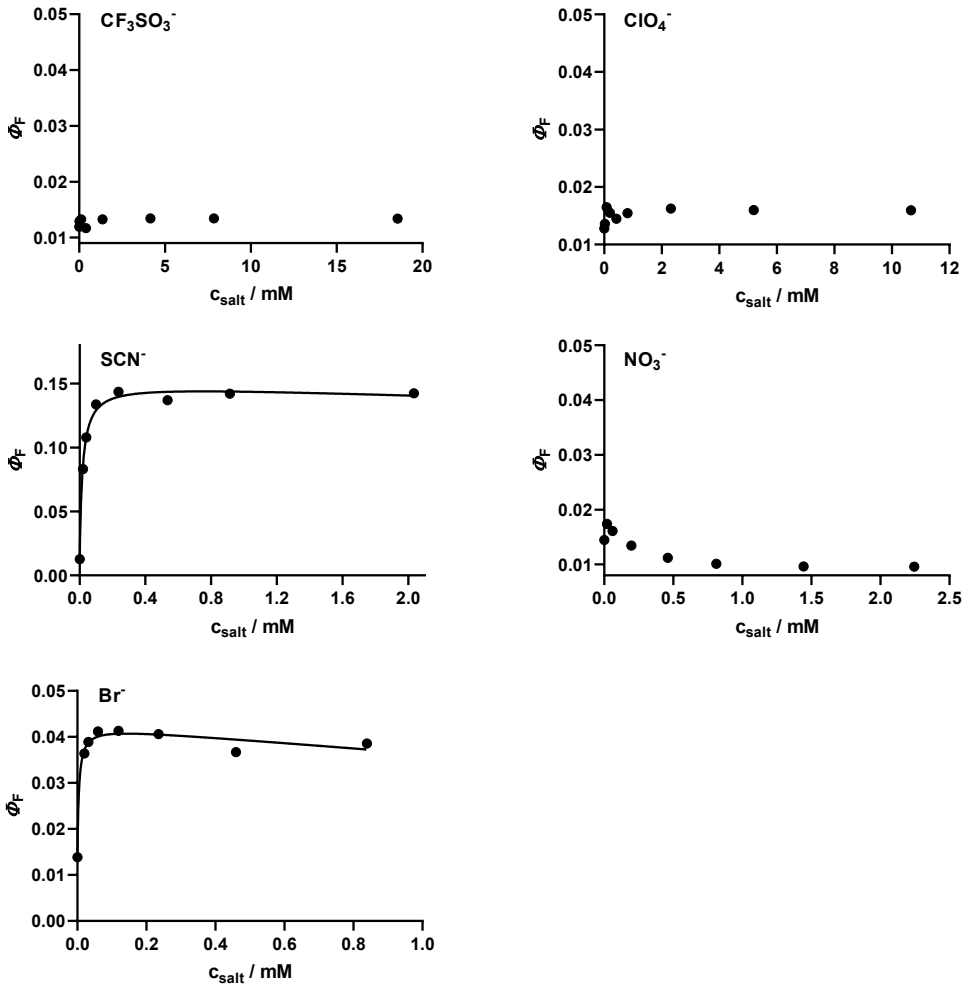

Fig. S11: The role of counter anions: Dependence of Φ_F of $\mathbf{3_B}$ in THF on the concentration of added sodium salt. The solid lines are the least-square fits to the experimental points.

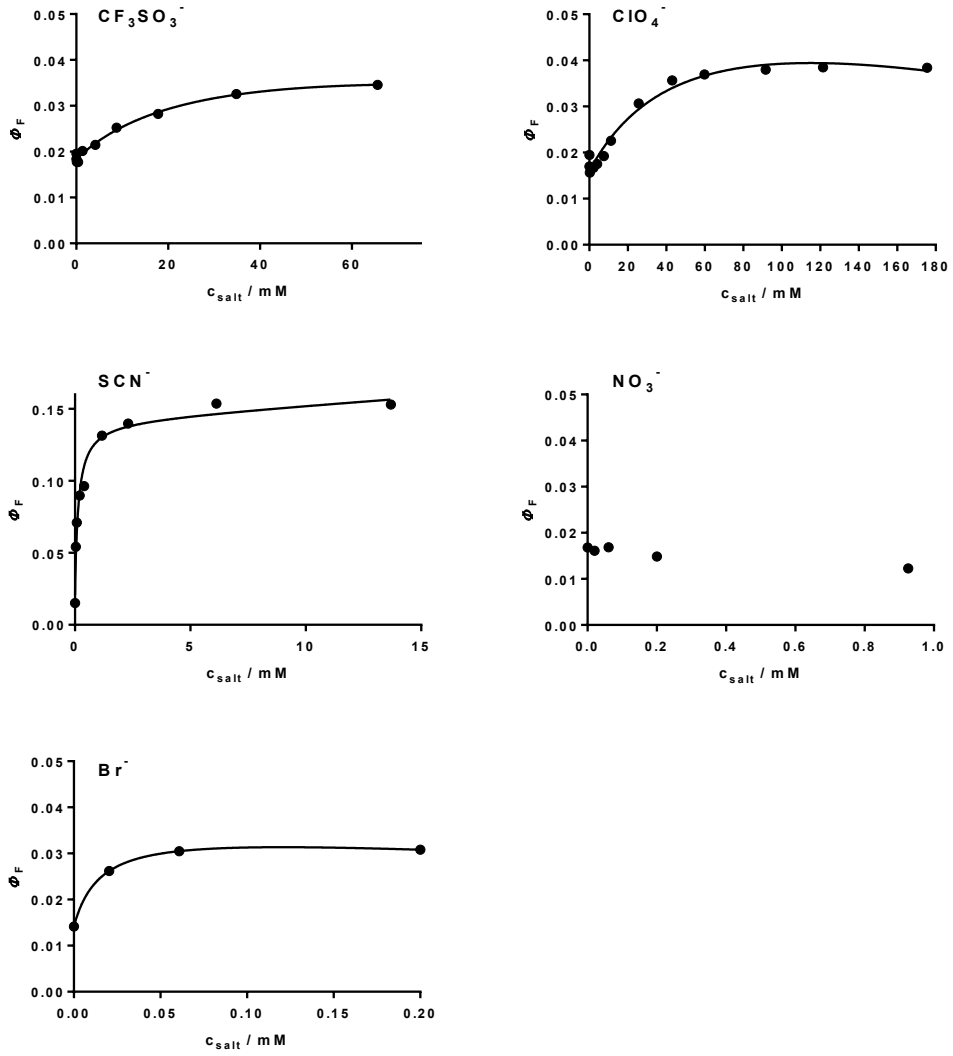

Fig. S12: The role of counter anion: Dependence of Φ_F of **5c** in THF on the concentration of added sodium salt. The solid lines are the least-square fits to the experimental points.

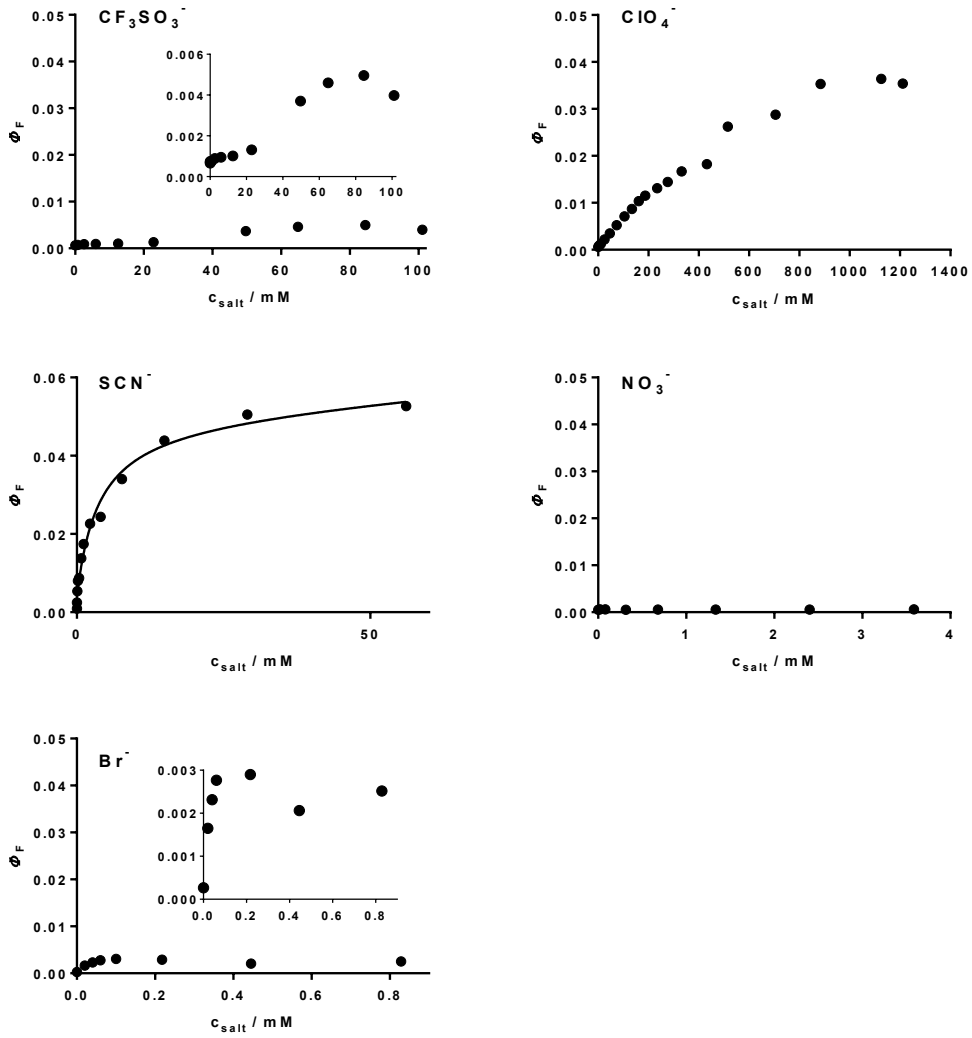

Fig. S13: The role of counter anion: Dependence of Φ_F of **8D** in THF on the concentration of added sodium salt. The solid line is the least-square fit to the experimental points.

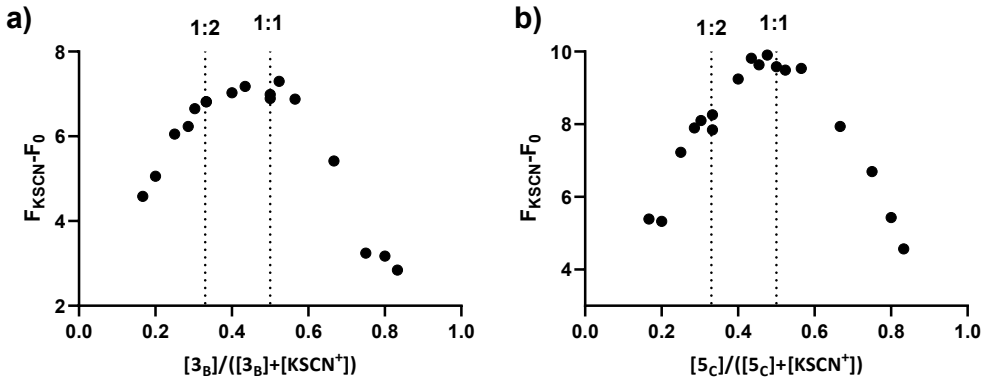

Fig. S14: Stoichiometry of binding KSCN with **3B** (a) and **5C** (b) assessed by Job method of continuous variation in THF.

Titration of control TPyzPzs **9Zn** and **9H** (without aza-crown moiety)

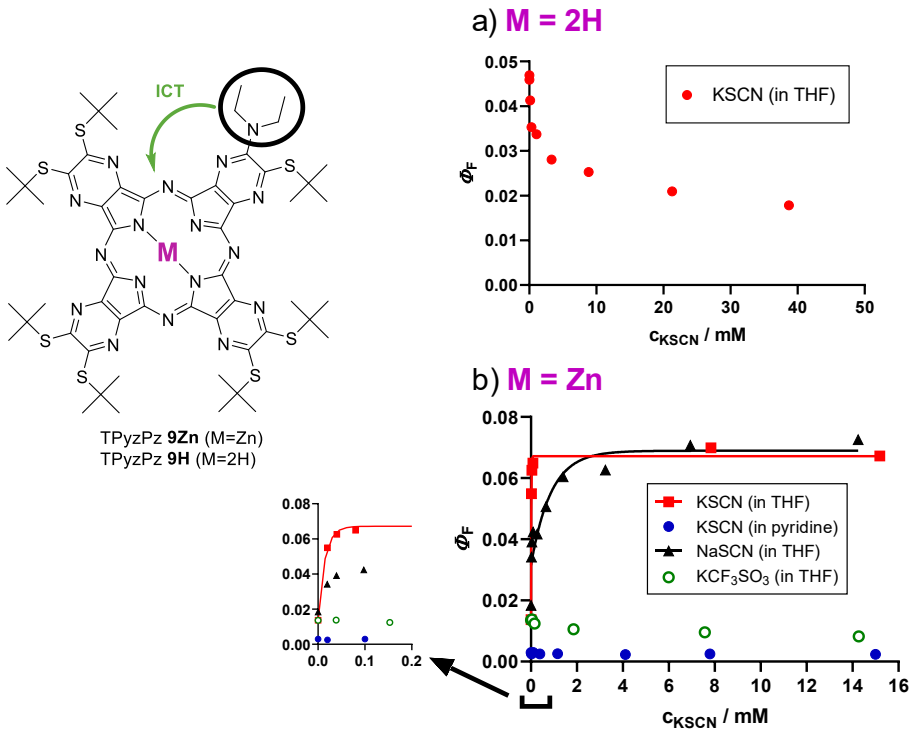

Fig S15: Dependence of Φ_F of control TPyzPz **9Zn** (b) and metal free analogue **9H** (a) in THF on concentration of added salt (excitation at 595 nm). The solid lines are the least-square fit to the experimental points.

MS spectra of mixtures of TPyzPzs $\mathbf{3_B}$, **9Zn** and **9H** with various salts

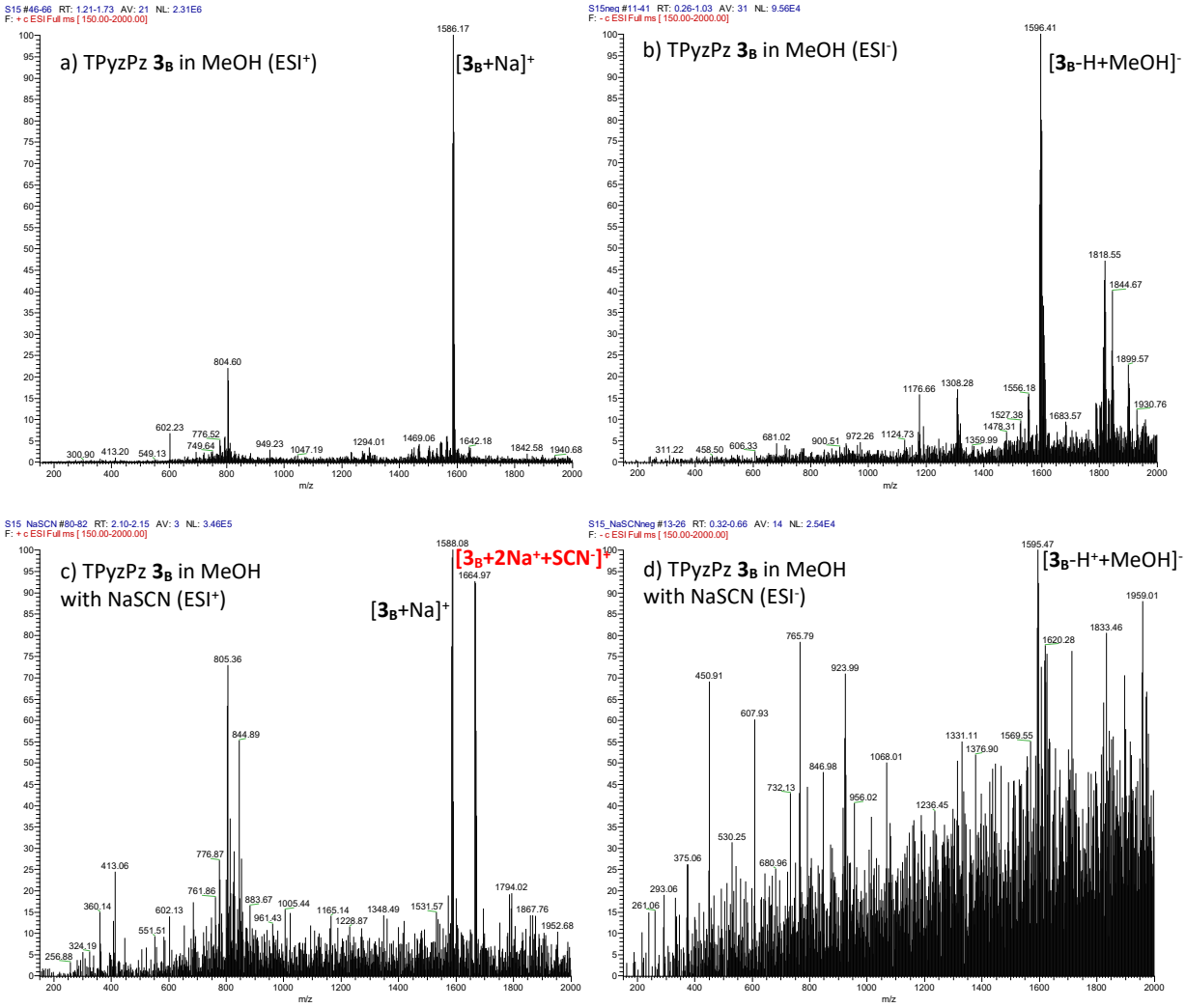

Fig. S16: MS spectra of TPyzPz $\mathbf{3_B}$ in MeOH taken in positive (ESI$^+$) (a, c) or negative (ESI$^-$) mode (b, d). MS spectra were taken before addition of NaSCN (a, b) after addition of NaSCN (ratio of TPyzPz/NaSCN 1:10)

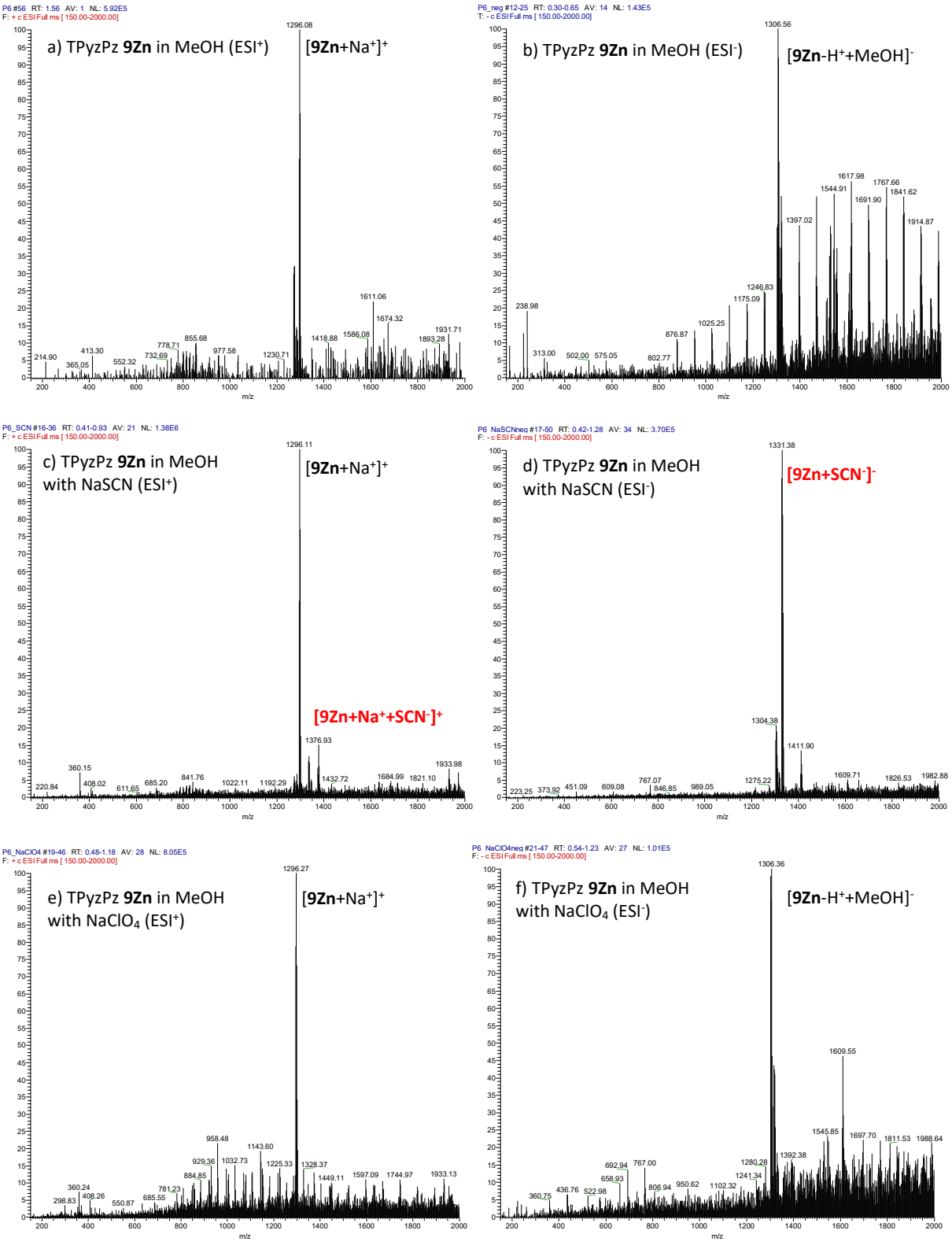
a) TPyzPz **9Zn** in MeOH (ESI+)
[**9Zn**+Na+]+
b) TPyzPz **9Zn** in MeOH (ESI-)
[**9Zn**-H+]-
c) TPyzPz **9Zn** in MeOH with NaSCN (ESI+)
[**9Zn**+Na+]+
[9Zn+Na+ +SCN-]+
d) TPyzPz **9Zn** in MeOH with NaSCN (ESI-)
[9Zn+SCN-]-
e) TPyzPz **9Zn** in MeOH with NaClO4 (ESI+)
[**9Zn**+Na+]+
f) TPyzPz **9Zn** in MeOH with NaClO4 (ESI-)
[**9Zn**-H+]-
m/z

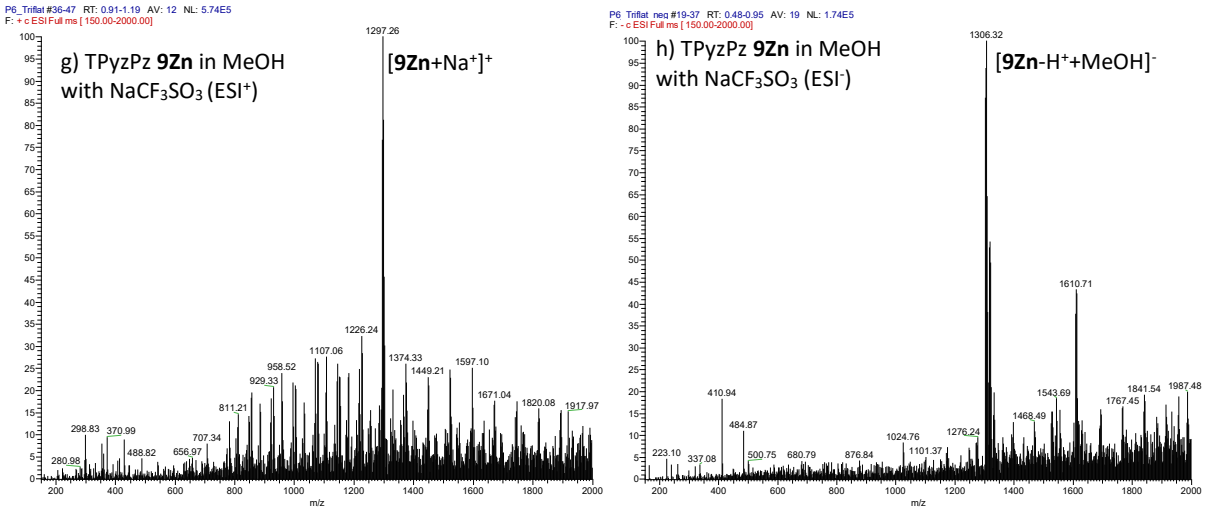

Fig. S17: MS spectra of TPyzPz **9Zn** in MeOH taken in positive (ESI^+) (a, c, e, g) or negative (ESI^-) mode (b, d, f, h). MS spectra were taken before addition of salt (a, b) after addition of particular salt (NaSCN, $NaClO_4$ or $NaCF_3SO_3$; ratio of TPyzPz/salt 1:10)

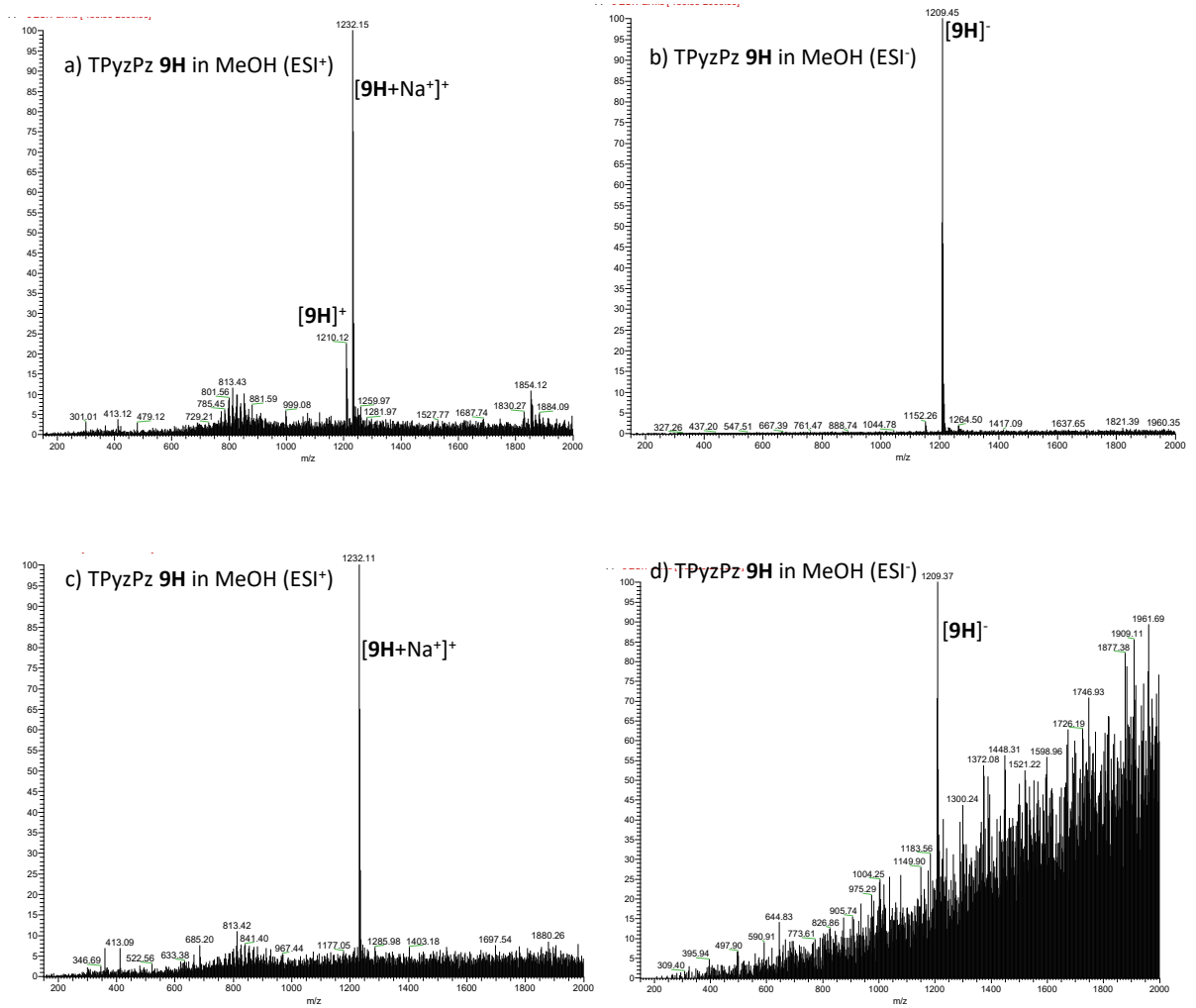

Fig. S18: MS spectra of metal-free TPyzPz **9H** in MeOH taken in positive (ESI^+) (a, c) or negative (ESI^-) mode (b, d). MS spectra were taken before addition of NaSCN (a, b) after addition of NaSCN (ratio of TPyzPz/NaSCN 1:10)

Titration experiments in water

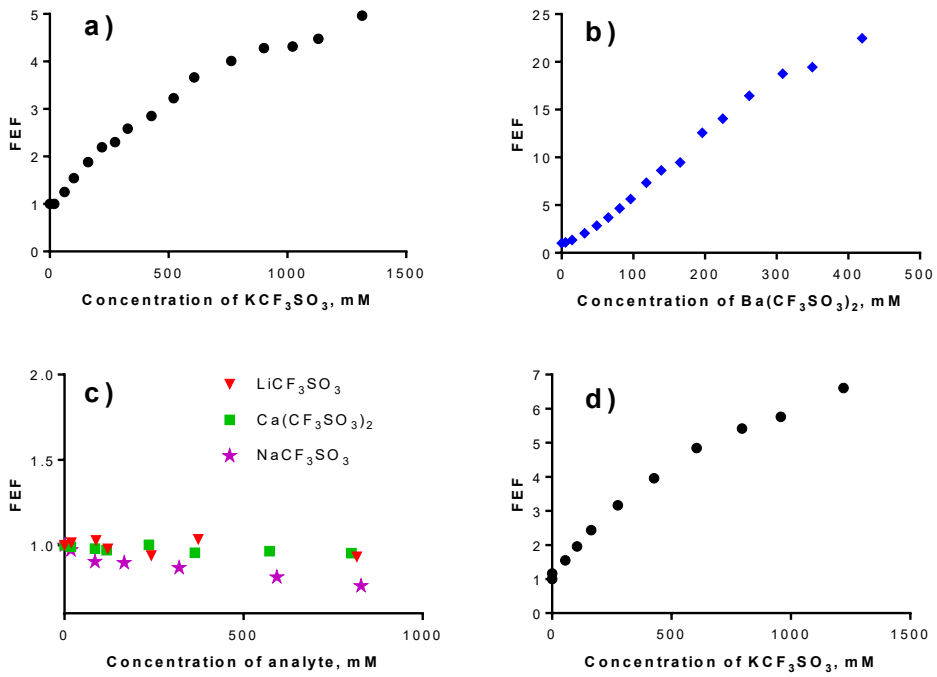

Fig S19: Increase of fluorescence of **3_B@NP** upon addition of different triflates in water (a) K^+, (b) Ba^{2+}, (c) insensitive analytes (Li^+, Ca^{2+} and Na^+), d) K^+ in the presence of 150 mM Na^+.

Characterization of prepared nanoparticles

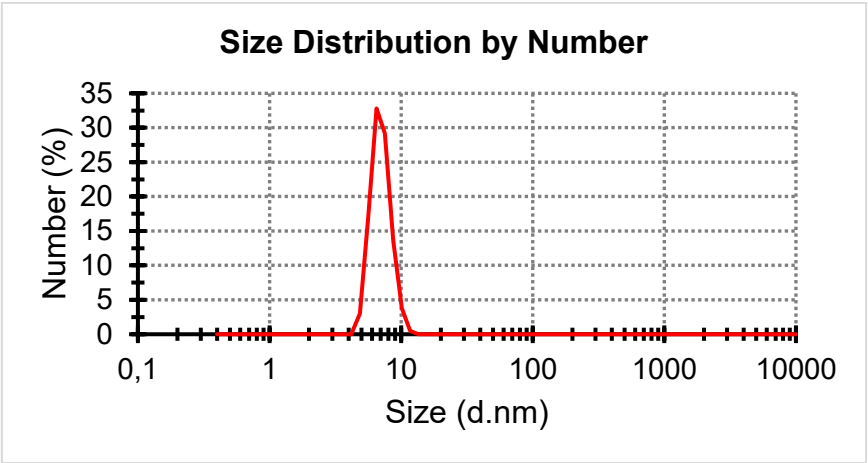

Fig. S20: Size distribution of **3_B@NP** obtained by DLS in water dispersions at room temperature.

Titration of TPyzPzs with KSCN

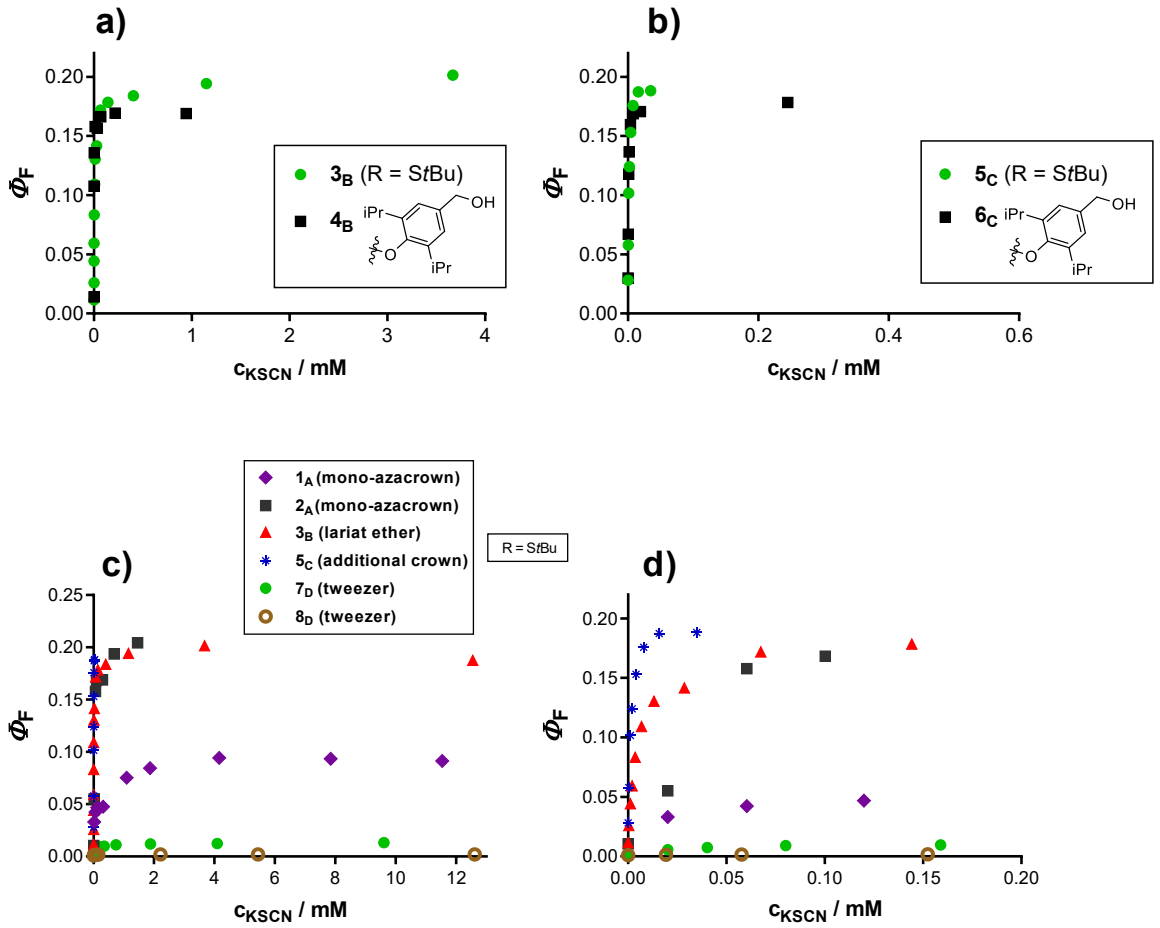

Fig. S21: Fluorescence response of TPyzPzs with recognition moiety B (a) and C (b) in THF upon addition of KSCN. Comparison of TPyzPzs with recognition moieties A, B, C and D (c). Graph (d) shows the enlarged area of graph (c).

Study of the sensitivity of $\mathbf{4_B}$ toward KSCN in EtOH/water solutions

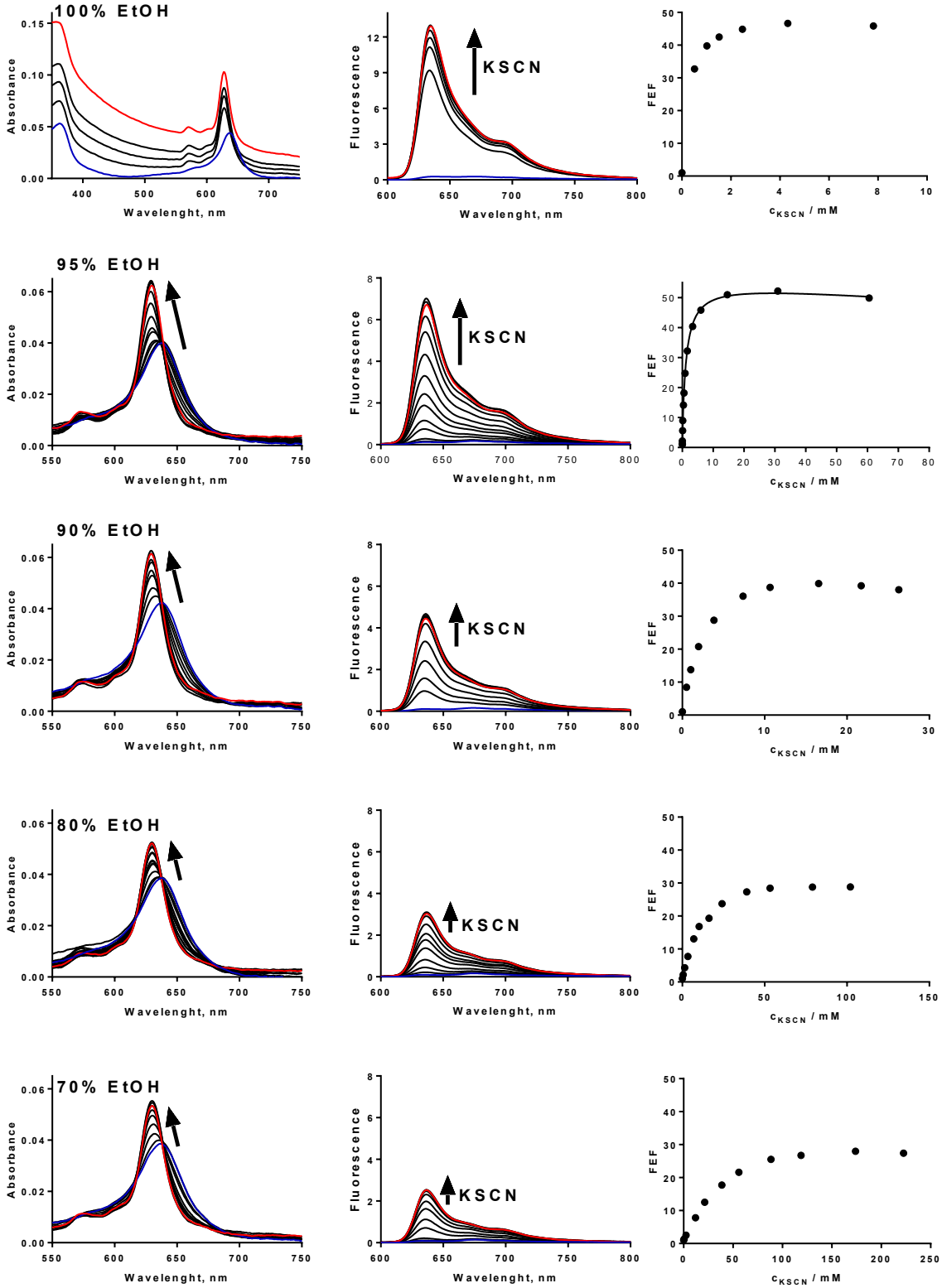

Fig. S22: Changes in absorption and emission spectra of $\mathbf{4_B}$ (1 µM) upon addition of KSCN. Right column represents appropriate FEF, the solid line is the least-square fit to the experimental points. Excitation wavelength was 580 nm.

Quantification of SCN^- in saliva

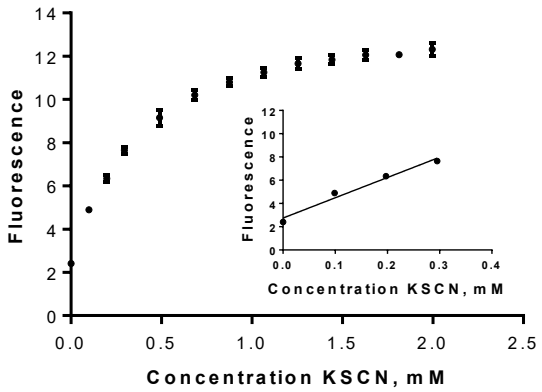

Fig. S23: Dependence of fluorescence intensity of $\mathbf{4_B}$ on the concentration of KSCN added in the saliva of a smoker. Data represent mean of three independent experiments. Inset depicts the linearity of the fluorescence intensity used for the quantification of SCN^- concentration by the method of standard addition. Excitation wavelength was 580 nm.

In vitro SCN^- sensing

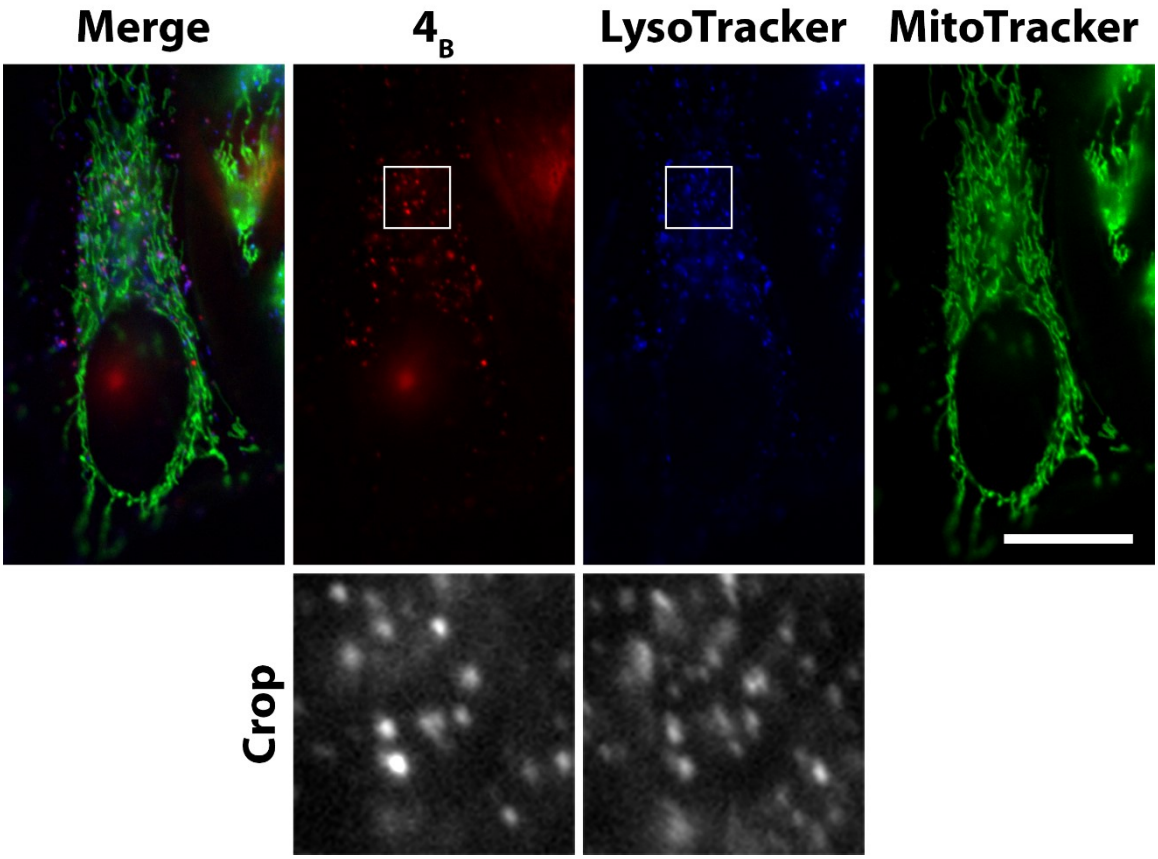

Fig. S24: Subcellular localization of $\mathbf{4_B}$ evaluated by fluorescence microscopy. Cells were stained with MitoTracker Green and LysoTracker Blue to visualize mitochondria and lysosomes, respectively. Crops of selected area (side of cropped area measures 10 µm) are presented as monochromatic images to better visualize the fluorescence signal. Bar represents 20 µm.

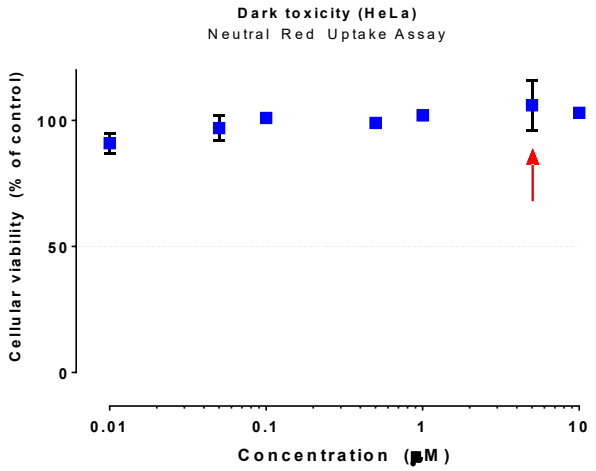

Fig. S25: Toxicity of $\mathbf{4_B}$ in the absence of light evaluated on HeLa cell line. Red arrow indicates the limit of solubility in cell culture media. Experiment was performed in triplicate.

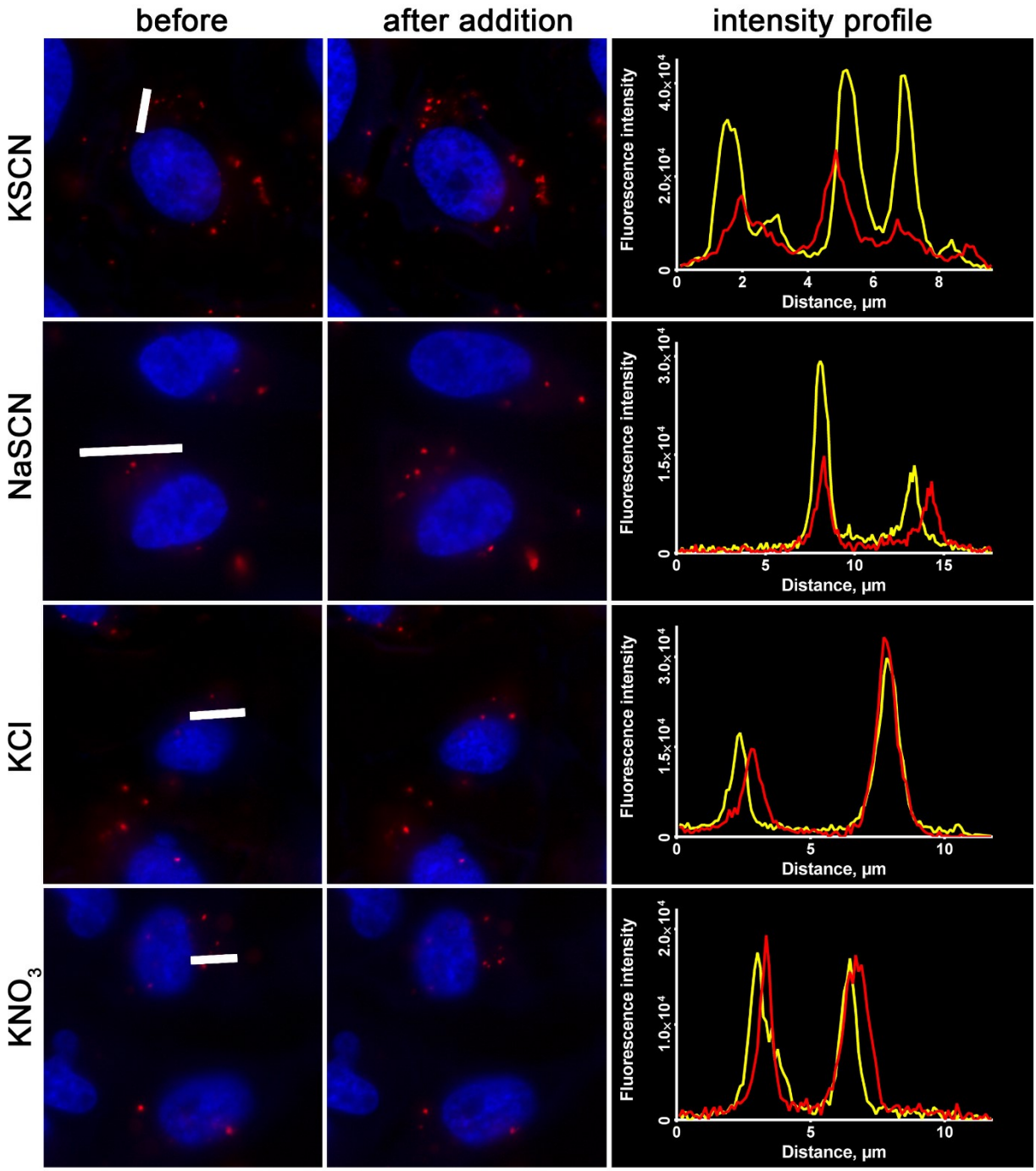

Fig. S26: Photomicrographs of HeLa cells stained for nuclei (blue, Hoechst 33342) and incubated with **6c** (5μM) (red) before and after addition of appropriate salts (NaSCN, KSCN, KCl, KNO_3) (10 mM). Red fluorescence intensity profiles correspond to the emission at respective white bars before addition of a salt; yellow fluorescence intensity profiles correspond to the emission at the same position after addition of a salt.

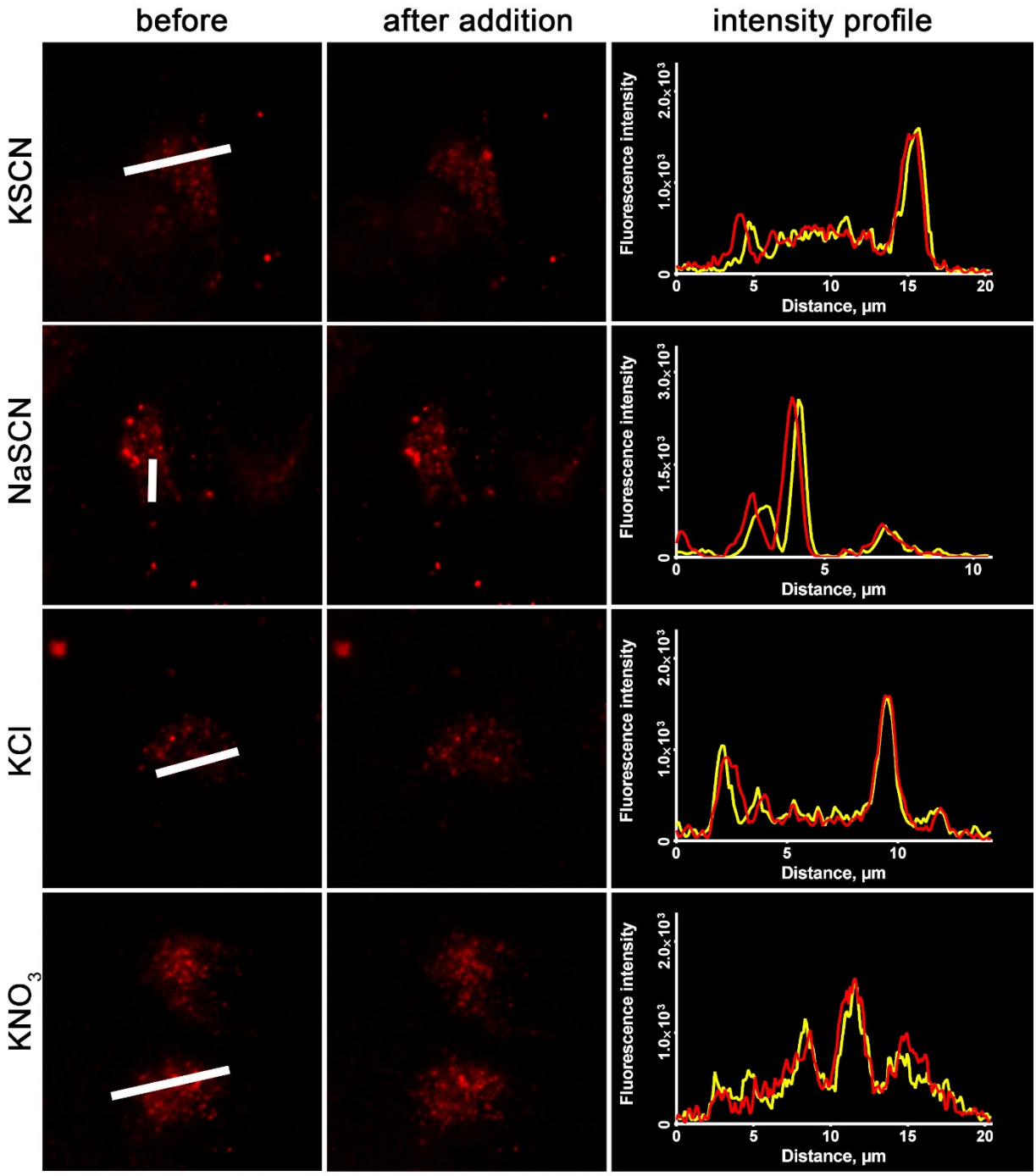

Fig. S27: Photomicrographs of HeLa cells incubated with always-ON control TPyzPz (i.e., always-ON control, structure shown in Fig. S28) (5μM) (red) before and after addition of appropriate salts (NaSCN, KSCN, KCl, KNO_3) (10 mM). Red fluorescence intensity profiles correspond to the emission at respective white bars before addition of a salt; yellow fluorescence intensity profiles correspond to the emission at the same position after addition of a salt.

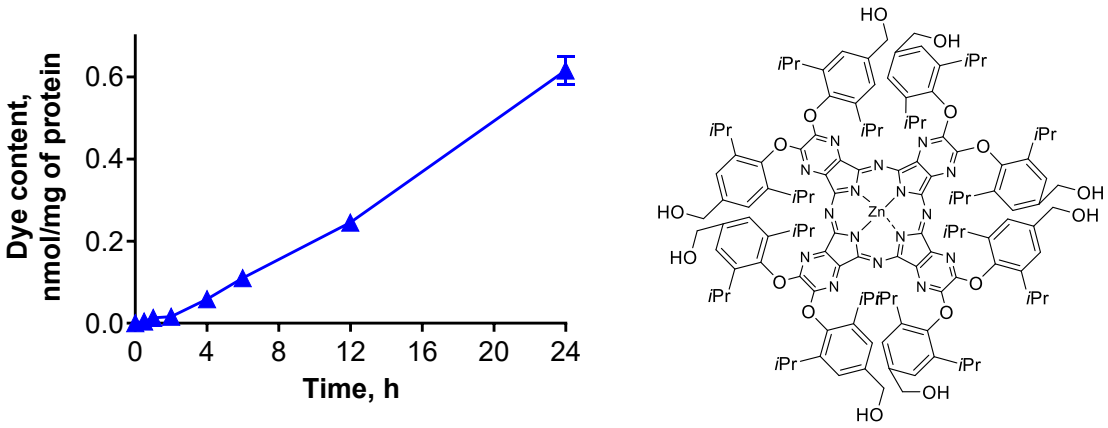

Fig. S28: Cellular uptake of always-ON control TPyzPz by HeLa cells after incubation with 0.5 µM of TPyzPz. The experiments were performed in duplicate.

References

1. Novakova, V.; Laskova, M.; Vavrickova, H.; Zimcik, P., Phenol-Substituted Tetrapyrazinoporphyrazines: pH-Dependent Fluorescence in Basic Media. *Chem. – Eur. J.* **2015,** 21, (41), 14382-14392.
2. Lochman, L.; Svec, J.; Roh, J.; Novakova, V., The role of the size of aza-crown recognition moiety in azaphthalocyanine fluorescence sensors for alkali and alkaline earth metal cations. *Dyes Pigm.* **2015,** 121, 178-187.
3. Novakova, V.; Lochman, L.; Zajícová, I.; Kopecky, K.; Miletin, M.; Lang, K.; Kirakci, K.; Zimcik, P., Azaphthalocyanines: Red Fluorescent Probes for Cations. *Chem. – Eur. J.* **2013,** 19, (16), 5025-5028.
4. Zimcik, P.; Miletin, M.; Novakova, V.; Kopecky, K.; Nejedla, M.; Stara, V.; Sedlackova, K., Effective Monofunctional Azaphthalocyanine Photosensitizers for Photodynamic Therapy. *Austr. J. Chem.* **2009,** 62, (5), 425-433.
5. Lochman, L.; Svec, J.; Roh, J.; Kirakci, K.; Lang, K.; Zimcik, P.; Novakova, V., Metal-Cation Recognition in Water by a Tetrapyrazinoporphyrazine-Based Tweezer Receptor. *Chem. - Eur. J.* **2016,** 22, (7), 2417-2426.
6. Novakova, V.; Zimcik, P.; Miletin, M.; Vachova, L.; Kopecky, K.; Lang, K.; Chábera, P.; Polívka, T., Ultrafast Intramolecular charge transfer in tetrapyrazinoporphyrazines controls the quantum yields of fluorescence and singlet oxygen. *Phys. Chem. Chem. Phys.* **2010,** 12, 2555-2563.
7. Zimcik, P.; Novakova, V.; Kopecky, K.; Miletin, M.; Uslu Kobak, R. Z.; Svandrlikova, E.; Váchová, L.; Lang, K., Magnesium Azaphthalocyanines: An Emerging Family of Excellent Red-Emitting Fluorophores. *Inorg. Chem.* **2012,** 51, (7), 4215-4223.